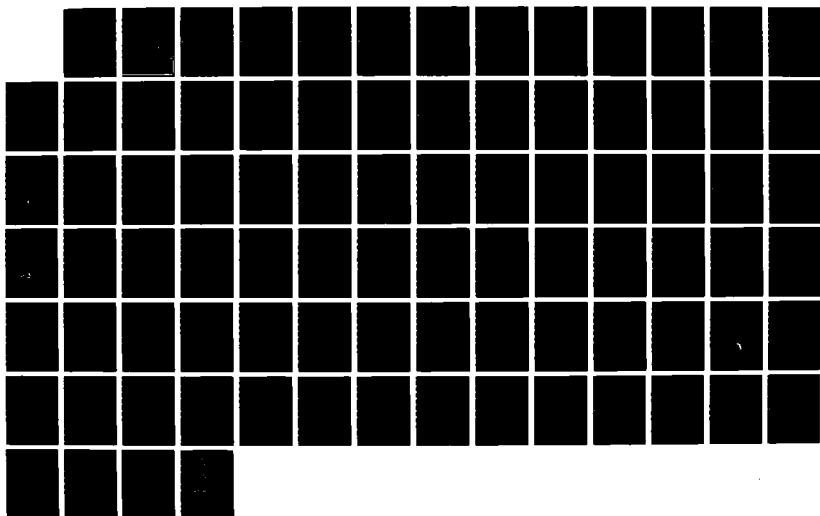
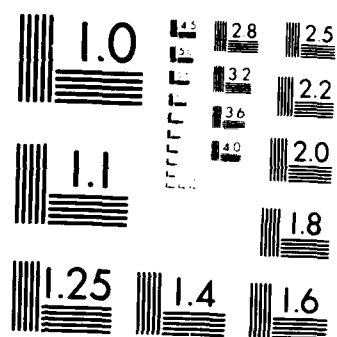


AD-A188 829

ORBITAL ANALYSIS OF A STS (SPACE TRANSPORTATION SYSTEM) 1/1
EXTERNAL TANK IN. (U) AIR FORCE INST OF TECH
WRIGHT-PATTERSON AFB OH SCHOOL OF ENGI.. D D MINER
DEC 87 AFIT/GA/RA/87D-4 F/G 22/3 ML

UNCLASSIFIED





MICROCOPY RESOLUTION TEST CHART
NATIONAL BUREAU OF STANDARDS-1963-A

AD-A188 829



DTIC FILE COPY

ORBITAL ANALYSIS OF A STS EXTERNAL TANK
IN LOW EARTH ORBIT

THESIS

Dennis D. Miner
Major, USAF

AFIT/GA/AA/87D-4



DTIC
ELECTE
FEB 08 1988
S H D

DEPARTMENT OF THE AIR FORCE
AIR UNIVERSITY
AIR FORCE INSTITUTE OF TECHNOLOGY

Wright-Patterson Air Force Base, Ohio

DISTRIBUTION STATEMENT A

Approved for public release;
Distribution Unlimited

88 2 03 059

AFIT/GA/AA/87D-4

ORBITAL ANALYSIS OF A STS EXTERNAL TANK
IN LOW EARTH ORBIT

THESIS

Dennis D. Miner
Major, USAF

AFIT/GA/AA/87D-4

DTIC
ELECTE
FEB 08 1988
H

Approved for public release; distribution unlimited

ORBITAL ANALYSIS OF A STS EXTERNAL TANK
IN LOW EARTH ORBIT

THESIS

Presented to the Faculty of the School of Engineering
of the Air Force Institute of Technology

Air University

In Partial Fulfillment of the
Requirements for the Degree of
Master of Science in Astronautical Engineering

Dennis D. Miner, B.S.

Major, USAF

December 1987

Accession For

NTIS GPO	✓
DTIC TAB	
Unannounced	
Justification	
By	
DTIC	
Approved	
Dissemination	
Dist	
A-1	

Preface

The idea behind this thesis came from articles printed in the bulletin of the Space Studies Institute of Princeton, New Jersey. The members of SSI have been most helpful in directing me to sources of information on the External Tank and its potential use in space.

In order to perform an orbital analysis a method of determining a satellite's position at some future time is required. A sophisticated orbit prediction computer program called the Artificial Satellite Analysis Program (ASAP) fulfills this need. I am grateful to my advisor, Captain Rodney Bain, for instructing me in its operation. His enthusiasm in the subjects of astrodynamics and celestial mechanics provided a key motivation for this work.

As section leader for GA-87D/88M, I would like to thank the other members for their help during our tour at AFIT and for their assistance in getting me up to speed after my twelve year academic layoff. And finally, I wish to express my love and respect to my wife, Gail, who has given steadfast support and encouragement during these challenging scholastic pursuits.

D. D. Miner

Table of Contents

	Page
Preface	ii
List of Figures	iv
List of Tables	v
Notation	vi
Abstract	viii
I. Introduction	1
II. Computer Programs	5
III. Orbit Perturbations	9
Gravitational	10
Atmospheric Drag	15
IV. Program Implementation	30
V. Results	34
VI. Conclusions and Recommendations	53
Appendix A: Conversion of the Spherical Harmonic to Keplerian Elements	58
Appendix B: Orbital Element Polynomials	67
Bibliography	69
Vita	72

List of Figures

Figure		Page
1.	Direct Injection	2
2.	Diurnal Atmospheric Bulge	17
3.	Atmospheric Density Variations with Altitude ..	19
4.	Velocity Notation	23
5.	Circular Cylinder Drag Coefficient	27
6.	STS External Tank	31
7.	Geocentric Altitude Fluctuations	35
8.	Linear Regression to Geocentric Altitude Data .	36
9.	Semi-Major Axis Time History	38
10.	Eccentricity Time History	39
11.	Inclination Time History	40
12.	Longitude of Ascending Node Time History	41
13.	Geocentric Altitude Time History	42
14.	Initial Altitude Effects on Orbit Decay	43
15.	Inclination Effects on Orbit Decay	44
16.	Eccentricity Effects on Orbit Decay	45
17.	Atmospheric Density Effects on Orbit Decay	48
18.	3-D Graph of 90-Day Altitude Loss	50
19.	Contour Graph of 90-Day Altitude Loss	51
20.	Multiple External Tanks	56
21.	Satellite Orbital Elements	60

List of Tables

Table	Page
I. Coefficients of Geopotential Harmonic	14
II. 90-Day Altitude Loss for Initial ET Altitudes ...	37
III. Air Drag/Gravity Field Coupling Effects	46
IV. Orbit Element Polynomials for Sun/Moon Effects ..	52

Notation

Symbol	Description
A	Satellite Area, normal to flow
a	Semi-Major Axis
a_e	Equatorial Radius of Primary
B	Ballistic Coefficient ($B = Cd A/2m$)
Cd	Coefficient of Drag
C_{1m}, S_{1m}	Spherical Harmonic Coefficients
D	Atmospheric Drag Force
e	Eccentricity
e_e	Ellipticity of Earth
f	True Anomaly
G	Universal Gravitational Constant
g	Acceleration Due to Gravity
H	Scale Height
i	Inclination
M	Mass of Primary
M	Mean Anomaly
m	Satellite Mass
R_e	Equatorial Radius of Earth
r	Radius from Center of Origin
r	Molecular Speed Ratio
t	Time (days)
V	Geopotential (per unit mass)

V	Velocity of Satellite Relative to Atmosphere
α	Right Ascension
α	Accommodation Coefficient
β	Inverse of Scale Height
ϕ	Latitude
λ	Longitude
μ	Earth Gravitational Parameter ($\mu = GM$)
ρ	Atmospheric Density
θ	Greenwich Sideral Time
Ω	Longitude of Ascending Node
ω	Argument of Periapsis
ω	Atmospheric Rotation Rate
ω_e	Rotation Rate of Earth

Abstract

By flying a different launch profile , it is possible for the Space Transportation System's Orbiter to bring the External Tank directly into space. Many studies by NASA and private industry have detailed the potential on-orbit uses of an External Tank. However, at Space Shuttle operating altitudes, an orbiting tank will experience multiple environmental forces resulting in its decay into the lower atmosphere and eventual re-entry.

This thesis conducts a preliminary study of a single External Tank in low Earth orbit. Criteria for a parking orbit are defined and, using an orbit prediction computer program with atmospheric drag and gravitational perturbations included, a search is made for the lowest initial altitude that will allow the External Tank to remain in this orbit window. The starting altitude that meets the orbit requirements is found to be within reach of the Shuttle's capabilities. The orbital elements of this parking orbit are then analyzed and a method for quick calculation of these parameters is devised. An evaluation of the factors that affect the orbital contraction of an External Tank is also performed. The atmospheric density and the tank characteristics can both contribute to high orbital decay rates.

ORBITAL ANALYSIS OF A STS EXTERNAL TANK IN LOW EARTH ORBIT

I. INTRODUCTION

One of the main goals of the Space Transportation System (STS) is to reduce the cost of delivering payloads into orbit. Reuse of the Solid Rocket Boosters and the Orbiter itself is a major factor in achieving this goal but the original Space Shuttle designers elected to make the External Tank (ET) an expendable element of the STS. Hence, on each flight, the ET is jettisoned by the Orbiter for a controlled entry into the Indian or Pacific Ocean. However, this component of the STS does not have to go to waste. When cast off, the External Tank has 98% of the energy needed to insert it into orbit. A more efficient launch trajectory, called direct injection, could be flown where the Space Shuttle Main Engines would boost the Orbiter with its attached External Tank into a standard Shuttle orbit (See Figure 1). The orbiter would then leave the ET and continue on its scheduled mission (8:1, I-1).

Why bring the External Tank into orbit? Many on-orbit applications of an ET have been proposed by government and private industry groups. This paragraph presents a review of

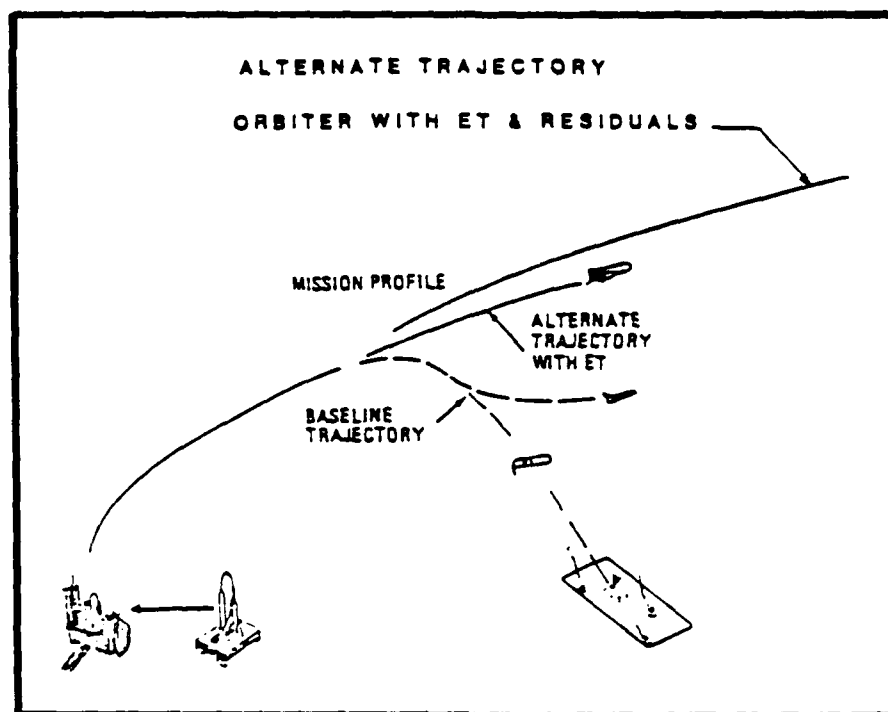


Figure 1. Direct Injection Trajectory

some of these proposals as discussed in Reference 8. The External Tank has approximately 53,000 lbs of aerospace grade aluminum. The tank could be disassembled in orbit with the pieces used to construct large space structures. It is also possible to melt the tank aluminum for on-orbit manufacturing uses, or leave the ET whole and use it as a basis for a space station. Each ET consists of a liquid hydrogen tank plus a smaller liquid oxygen tank; both capable of on-orbit storage of cryogenic fuels and other volatiles. Studies have been done to investigate the employment of tethers in space. The potential uses of the ET connected to a tether range from

momentum exchange with the Shuttle to electrical generation with a conducting tether. However, prior to utilizing an External Tank in space, a major obstacle must be addressed; how to prevent it from decaying out of orbit prematurely.

All objects in low Earth orbit (LEO) experience atmospheric drag. Work is required to push the air molecules out of the way which reduces the kinetic energy of a satellite. This effort causes the orbit to shrink where the orbital velocity requirement is greater. This increase in speed combined with the higher density of the lower atmosphere results in an increased drag force. And the cycle continues until the satellite falls out of orbit (25:296). This phenomena was observed with the Skylab space station. Skylab's orbit decayed due to increased solar activity that affected the density of the atmosphere. The additional drag on the spacecraft led to its earlier than planned re-entry (24:39). An orbiting External Tank would suffer the same fate. An unexpected re-entry would defeat the purpose for bringing the ET into space and produce the possibility of raining large pieces of a disintegrating tank over populated areas. A method of orbit maintenance is desirable but the first tanks taken into orbit may not be equipped with small thrusters to accomplish this task. And possibly, ET end-users would make use of the tank before it began a final, blazing plunge through the lower layers of the atmosphere.

The thrust of this thesis is to determine a parking orbit for a single External Tank, awaiting its future

purpose. Two qualifying assumptions are made to form a basis for this investigation. First, the time horizon chosen is 90 days. This three month window is selected to represent the amount of time allowed for the ET to remain in its parking orbit. It is also assumed that the maximum tolerable altitude loss by the ET over the 90-day period would be 25 kilometers. These two assumptions thus produce a platform from which to answer the primary question: What is the lowest initial altitude for deploying the External Tank sufficient to meet this parking orbit requirement?

An orbit prediction computer program, coupling a gravitational field and a simple atmosphere model, is employed for this External Tank orbital analysis. Typical Shuttle orbit parameters of 28° inclination and zero eccentricity (circular orbit) are used in the search for a minimum parking orbit. The Keplerian elements a, e, i, Ω and the geocentric altitude of this orbit are then analyzed over the 90-day period and a simple method is devised allowing quick calculation of these ET orbital parameters. Finally, various aspects of the orbit, Earth's gravitational field and atmosphere, and External Tank properties are investigated to determine their relationship with orbital decay. Chapter V details the results of this examination of an External Tank in low Earth orbit.

II. COMPUTER PROGRAMS

Several computer programs were used in formulating and analyzing the External Tank orbital data. The data itself was generated by the Artificial Satellite Analysis Program (ASAP) from Reference 16 while data analysis and graphing was accomplished using various programs and software packages.

Artificial Satellite Analysis Program (ASAP)

ASAP is a general orbit prediction program written in the standard ANSI 77 FORTRAN language. Though originally configured to run on an IBM microcomputer, ASAP was converted to operate on AFIT's mainframe systems. This program uses Cowell's method of special perturbations in formulating the differential equations of motion (EOM).

Cowell's method works with cartesian coordinates (x,y,z) and their time derivatives $(\dot{x},\dot{y},\dot{z})$. The EOM can be expressed as

$$\begin{aligned}\dot{x} &= V_x \\ \dot{y} &= V_y \\ \dot{z} &= V_z \\ \ddot{x} = \dot{V}_x &= -\mu \frac{x}{r^3} + \text{perturbations} \\ \ddot{y} = \dot{V}_y &= -\mu \frac{y}{r^3} + \text{perturbations} \\ \ddot{z} = \dot{V}_z &= -\mu \frac{z}{r^3} + \text{perturbations} \quad (1)\end{aligned}$$

where

$$r = (x^2 + y^2 + z^2)^{1/2}$$

$$\mu = G M$$

ASAP's numerical integrator requires the equations of motion be written as a system of 6 first order differential equations. The integrator is an 8th order Runge-Kutta single step integration scheme with variable step-size control. The perturbations handled by ASAP include the primary body disturbing function, atmospheric drag and solar/lunar effects. For the sake of completeness, a general discussion of the gravitational and atmospheric drag perturbations is provided in Chapter III. The method of their implementation in ASAP is then covered in Chapter IV.

In addition to basic constants for the central planet the following are user inputs to ASAP:

- 1) Coefficients of Spherical Harmonics
- 2) Atmospheric Data
 - A) Reference Altitude (km)
 - B) Scale Height at Reference Altitude (km)
 - C) Density at Reference Altitude (kg/km^3)
- 3) Satellite Data
 - A) Area, normal to flow (km^2)
 - B) Mass (kg)
 - C) Coefficient of Drag
- 4) Initial Orbital Elements
 - A) Semi-Major Axis (km)
 - B) Eccentricity
 - C) Inclination (deg)
 - D) Longitude of Ascending Node (deg)
 - E) Argument of Periapsis (deg)
 - F) Mean Anomaly (deg)

- 5) Starting Day and Time
- 6) Stopping Day and Time
- 7) Time Step

At each time step ASAP integrates the equations of motion, Eqs (1), and calculates the Keplerian elements. Since perturbations have been included in the EOM, the orbital elements will not remain constant but be functions of time. The orbit described by these elements is the two body orbit a satellite would follow if all the perturbations were removed at that moment in time (28:29-30). These instantaneous values of the orbital elements are used as a basis for calculating the satellite's orbit parameters at the next time period. At each step ASAP generates the following output:

- 1) Day
- 2) Hour
- 3) Semi-Major Axis (km)
- 4) Eccentricity
- 5) Inclination (deg)
- 6) Longitude of Ascending Node (deg)
- 7) Argument of Periapsis (deg)
- 8) Mean Anomaly (deg)
- 9) Geocentric Altitude (km)

Other Programs

The Artificial Satellite Analysis Program, as it calculates the orbital elements, produces an ASCII file which can be imported to spreadsheet type software. The database management capabilities of this program allows rapid analysis of the orbital parameters. For the External Tank orbit study a two hour time step was employed which produced

12 orbit element calculations per day for the three month period. The value of the parameters at the zero hour of each day was extracted for integration into the graphics portion of the software. The orbital element time histories were produced with this data. A linear regression function was another program feature used. As will be discussed in Chapter V, this capability provided a convenient method for defining the altitude loss rate.

In addition to the spreadsheet program, a modification to a FORTRAN program from Reference 7 was developed to calculate multiple order least squares polynomials. This technique was used to 'average' the daily changes in the orbital elements thereby exposing their long period behavior.

III. ORBIT PERTURBATIONS

A satellite, orbiting a spherical planet of homogeneous structure and with no outside environmental disturbances, would continue forever in an idealized Keplerian orbit; its orbital elements remaining constant at their initial values. In real celestial systems however, there are interfering influences capable of perturbing the satellite's motion:

- 1) the irregular shape and variable composition of the primary
- 2) the atmosphere of the primary
- 3) the magnetic field of the primary
- 4) the solar radiation pressure
- 5) the gravitational fields of other nearby bodies

This thesis will concern itself primarily with the first two perturbations listed.

The magnitude of a perturbing force gives no hint as to its effect on a specific orbital element (9:973). For instance, the Earth's gravitational attraction is on the order of one dyne, but because it is a conservative force, produces no appreciable long term perturbation upon a satellite's semi-major axis. Conversely, the atmospheric drag (on the order of 10^{-5} dyne) acting on a low orbit satellite causes a noticeable secular decrease in the semi-major axis.

The next two sections will discuss in detail the two principal perturbations experienced by a satellite in low Earth orbit.

Gravitational Perturbations

As experienced by a satellite in low orbit, Earth's gravitational field does not exhibit spherical symmetry. The equatorial bulge, continent land masses and irregular ocean floors all contribute to Earth's deviation from a Newtonian point mass and produce a non-spherical shape to Earth's gravitational field (28:48). As a satellite circles the globe it encounters a variable force of gravity leading to changes in its orbital parameters. A formulation is needed to model this perturbing effect.

The attractive force between two bodies of mass M and m , separated by distance r , is governed by Newton's universal law of gravity:

$$F = G \frac{M m}{r^2} \quad (2)$$

Combining Eq (2) with Newton's second law

$$F = m a \quad (3)$$

provides the acceleration of body m with respect to the two-body system's center of mass:

$$a = \frac{G M}{r^2} \quad (4)$$

For the case where $m \ll M$, the two-body system's center of mass can be conveniently considered at the center of body M . Instead of working with an acceleration in determining the gravitational disturbance, it is simpler to convert the

acceleration to a vector and express this vector as a potential function (14:1-2).

The vector \bar{a} is obtained by representing the acceleration as a gradient of a scalar, V , defined as the potential (per unit mass):

$$\bar{a} = \nabla V \quad (5)$$

where

$$V = \frac{G M}{r} \quad (6)$$

This acceleration \bar{a} is used in developing Poisson's fundamental partial differential equation for gravitational fields (6:277,279):

$$\nabla^2 V = - 4 \pi G \rho \quad (7)$$

where ρ = density of M . For a satellite orbit outside the body M , the density equals zero which leads to Laplace's equation:

$$\nabla^2 V = 0 \quad (8)$$

In rectangular coordinates, Laplace's equation becomes

$$\nabla^2 V = G M \left[- \frac{3}{r^3} + \frac{3(x^2 + y^2 + z^2)}{r^5} \right] = 0 \quad (9)$$

Since the body M (Earth, in this case) is basically spherical in shape, transforming Eq (9) into spherical coordinates will aid in the derivation. This can be accomplished with

$$\begin{aligned} x &= r \cos\phi \cos\lambda \\ y &= r \cos\phi \sin\lambda \\ z &= r \sin\phi \end{aligned} \quad (10)$$

where

r = radial distance from coordinate frame origin

ϕ = latitude

λ = longitude

Thus, Laplace's equation transforms to (13:2-3)

$$r^2 \nabla^2 V = \frac{\partial}{\partial r} \left[r^2 \frac{\partial V}{\partial r} \right] + \frac{1}{\cos \phi} \frac{\partial}{\partial \phi} \left[\cos \phi \frac{\partial V}{\partial \phi} \right] + \frac{1}{\cos^2 \phi} \frac{\partial^2 V}{\partial \lambda^2} \quad (11)$$

Any solution V to Eq (11) is referred to in literature as a spherical harmonic but a closed form solution does not exist. Instead, a general infinite series expansion for V can be derived (14:4-6):

$$V = \sum_{l=0}^{\infty} \sum_{m=0}^l r^{-l-1} P_{lm}(\sin \phi) \left[C_{lm} \cos m\lambda + S_{lm} \sin m\lambda \right] \quad (12)$$

Eq (12) involves an associated Legendre function:

$$P_{lm}(\sin \phi) = \cos^m \phi \sum_{t=0}^k T_{lmt} \sin^{l-m-2t} \phi \quad (13)$$

where k = integer part of $(l-m)/2$ and

$$T_{lmt} = \frac{(-1)^t (2l-2t)!}{2^l t! (l-t)! (l-m-2t)!} \quad (14)$$

The constants C_{lm} and S_{lm} characterize the mass distribution of body M and the terms l and m are the order and degree of the potential. In this thesis the notation 3x3 refers to a potential of order 3 and degree 3. To represent a model of the Earth's geopotential, Eq (12) can be expressed as (6:284)

$$V = \frac{\mu}{r} \sum_{l=0}^{\infty} \sum_{m=0}^l \left(\frac{R_e}{r} \right)^l P_{lm}(\sin\phi) [C_{lm} \cos m\lambda + S_{lm} \sin m\lambda] \quad (15)$$

By including the Earth's gravitational parameter μ and equatorial radius R_e , C_{lm} and S_{lm} are redefined from Eq (12) to make them dimensionless.

When $m = 0$ Eq (15) simplifies to

$$V = \frac{\mu}{r} \sum_{l=0}^{\infty} \left(\frac{R_e}{r} \right)^l P_{l0}(\sin\phi) [C_{l0}] \quad (16)$$

The geopotential components of this equation are referred to as zonal harmonics and are due to variations in meridian ellipticity. When $m = 1$, the components of Eq (15) are called sectoral harmonics and are caused by longitudinal variations in the shape of the Earth. Tesseral harmonics are concerned with cases where $m < l$ (6:271). (Note: For all $m > l$, the associated Legendre function $P_{lm}(\sin\phi)$ equates to zero.) Values of the potential coefficients C_{lm} and S_{lm} for Earth were determined from repeated observations of various satellite orbits. By studying the long term perturbations, the coefficients of the zonal harmonics have been found and the sectoral and tesseral harmonic coefficients were discovered from analysis of short term orbit perturbations. These geopotential constants have been calculated through many orders and degrees.

The 3x3 geopotential coefficients of concern to this thesis are listed in Table I (6:285).

TABLE I

Coefficients of Geopotential Harmonics

l	$C_{10} \times 10^6$	l	m	$\bar{C}_{1m} \times 10^6$	$\bar{S}_{1m} \times 10^6$
2	-1082.645	2	2	2.379	-1.351
3	2.546	3	1	1.936	0.266
		3	2	0.734	-0.538
		3	3	0.561	1.620

When both l and m equal zero, Eq (15) reduces to the basic potential for a spherically symmetric Earth:

$$V = \frac{\mu}{r} = \frac{G M}{r} \quad (6)$$

meaning $C_{00} = 1$ and $S_{00} = 0$ (28:56). By placing the coordinate frame at the center of the Earth, coefficients C_{10} , C_{11} , S_{11} will be zero and, from empirical data, C_{21} and S_{21} have been shown to be exceedingly small (6:285). The sectoral and tesseral harmonic coefficients \bar{C}_{1m} and \bar{S}_{1m} in Table I are related to the constants C_{1m} and S_{1m} of Eq (15) by

$$\begin{aligned} C_{1m} &= T \bar{C}_{1m} \\ S_{1m} &= T \bar{S}_{1m} \end{aligned} \quad (17)$$

where

$$T = \left[\frac{2 (2l+1) (l-m)!}{(l+m)!} \right]^{1/2} \quad (18)$$

At this stage the geopotential has been developed into a form used by the Artificial Satellite Analysis Program. As it is of interest to this thesis to examine the long period

perturbating effects of Earth's gravitational field, the time histories of the External Tank orbital elements are generated by ASAP and then a curve fitting to this data is performed. This approach to determine the long term trends is a reverse procedure from an analytical technique called the method of averages (12:1). In this process the disturbing function, i.e., the geopotential, is averaged prior to its use in the equations of motion. This is accomplished by using

$$\langle V_{ave} \rangle = \frac{1}{2\pi} \int_0^{2\pi} V(M) dM \quad (19)$$

where the potential is averaged over one orbit period (13:3). However, as Eq (15) now stands, the geopotential is a function of radius r , latitude ϕ and longitude λ . For use in the method of averages it is necessary to convert Eq (15) to the Keplerian elements a, e, i, Ω, ω and M . This conversion is presented in Appendix A.

Atmospheric Drag Perturbations

As a satellite passes through the rarified regions of the upper atmosphere it is subjected to an aerodynamic force which perturbs its orbital motion. This force can be separated into two quantities: (1) the component opposite the direction of motion called drag, (2) the component perpendicular to the satellite's flight path. This second quantity generally does not pass through the satellite's

center of mass and can subsequently be divided into a lifting force and a turning moment about the center of mass. According to Reference 15 the aerodynamic lift can be neglected in an orbital analysis as the lift to drag ratio for satellites is very small (<0.1). Also, if uncontrollable, a satellite would rotate the lift vector through all possible directions over a period of time thus producing a resultant force of zero. These assumptions for ignoring the lift force are particularly reasonable for cylindrical satellites with length to diameter ratios greater than 1 (15:13). (The ratio of l/d for the External Tank is 5.6.) In addition, a cylindrical satellite in a gravity gradient orientation with its longitudinal axis pointing at the Earth's center would not generate any lift.

In aerodynamics the conventional drag equation is

$$D = 1/2 \rho V^2 C_d A \quad (20)$$

where

D = drag force

ρ = atmospheric density

V = satellite velocity relative to the atmosphere

C_d = drag coefficient

A = satellite area normal to air flow

This formulation of the drag equation can alternately be expressed as a drag deceleration:

$$\frac{D}{m} = \frac{C_d A}{2m} \rho V^2 = B \rho V^2 \quad (21)$$

The ballistic coefficient B is a convenient method of combining the satellite parameters (A, m, C_d) into one term for parameteric studies (11:183-184).

The elements of the drag equation will now be examined with respect to an Earth orbiting spacecraft.

Atmospheric Density. The major property of the Earth's atmosphere important to low orbit satellites is its density. The density in the upper regions of the atmosphere is an exceedingly variable quantity with solar activity being the main cause of this irregularity. Observations of the orbits of early satellites were used in analyzing these atmospheric density fluctuations. (9:978-979).

One basic air density difference exists between the sunlit and nighttime sides of the Earth. See Figure 2 from Reference 11. This hump of density, the diurnal bulge,

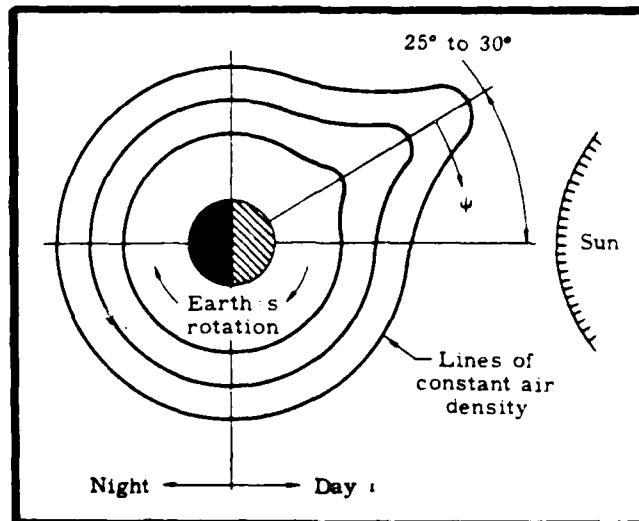


Figure 2. Diurnal Atmospheric Bulge

occurs about two hours after midday. The change in density between day and night is small for altitudes of 250 km and below, however, above this altitude large variations can take place. For example, at 600 km, the maximum daytime density is about 8 times greater than the nighttime minimum (15:18).

Along with this daily density variation there are four other solar influences. First, there exists an irregular day-to-day deviation in density due to ephemeral solar disturbances such as short term flares. A second density variation occurs with a 27-day cycle. This effect is due to the axial rotation of the Sun with respect to the Earth. Next, the properties of the atmosphere also respond to the 10-11 year sunspot cycle. And fourth, a seasonal oscillation in density appears with a minimum occurring during July and January and a maximum appearing in October and April. These seasonal effects are largely due to the Earth's orbit around the Sun (15:18-19).

Through many orbital studies of Earth satellites the atmosphere and its properties have been analyzed in much detail. From these observations the atmospheric density has shown to vary exponentially (as a first approximation) with height (15:20,22). Figure 3 is a logarithmic plot of air density versus altitude that demonstrates this effect (21:20). The relatively straight line relationship between 200 and 800 km allows the atmospheric density to be expressed by a simple exponential law (15:22):

$$\rho = \rho_0 \exp [-(h-h_0)/H] \quad (22)$$

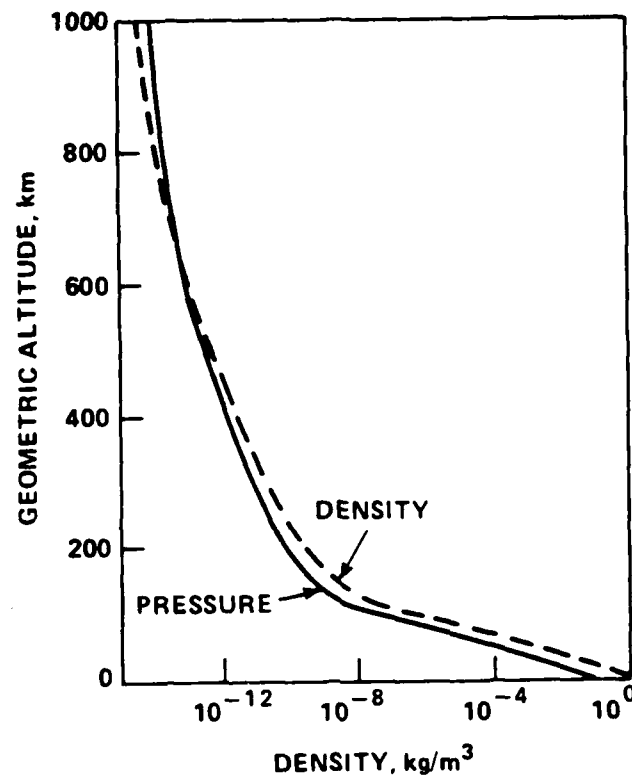


Figure 3. Atmospheric Density Variation with Altitude

where

- h \equiv altitude
- h_0 \equiv reference altitude
- ρ_0 \equiv density at reference altitude
- H \equiv scale height

The scale height is the vertical distance in which the air density changes by a factor of exponential e (22:233). The value of H is dependent on altitude, increasing slowly with height. H can be derived in the following manner (27:4).

Two basic equations play a part in determining air density as a function of altitude. First, the perfect gas

law relates the atmospheric properties pressure P , density ρ and temperature T :

$$P = \rho \frac{R^*}{M} T \quad (23)$$

where

$R^* \equiv$ universal gas constant

$M \equiv$ mean molecular weight of the atmosphere

The second expression is the hydrostatic equation which relates the rate of change in pressure to the increased weight of the supported atmosphere:

$$dP = - \rho g dr \quad (24)$$

where $g \equiv$ gravitational acceleration. Logarithmic differentials of Eq (23) give

$$\frac{d\rho}{\rho} = \frac{dP}{P} - \frac{dT}{T} \quad (25)$$

When combined with Eq (24) this produces

$$\frac{d\rho}{\rho} = - \left[\frac{g M}{R^* T} + \frac{1}{T} \frac{dT}{dr} \right] dr \quad (26)$$

or

$$\frac{d\rho}{\rho} = - \beta dr \quad (27)$$

where β is the terms in the brackets of Eq (26) and represents the inverse of the scale height. Integrating Eq (27) and substituting H for $1/\beta$ yields the density exponential equation Eq (22).

Several different density profiles can be considered depending on assumptions on β (27:4-5):

1) Strictly exponential atmosphere: β is assumed constant throughout the atmosphere.

2) Locally exponential atmosphere: β is constant over a small altitude window.

3) βr - constant atmosphere: The dimensionless quantity βr remains constant.

4) Isothermal atmosphere: The temperature is considered constant through an altitude interval so that $dT/dr = 0$ and β becomes gM/R^*T . For an inverse-square gravitational field

$$g = g_0 [r_0/r]^2 \quad (28)$$

which leads to the quantity βr^2 being constant.

All four profiles use the density exponential function of Eq (22).

The biggest limitation in using this atmospheric model is the assumption of spherical symmetry. As expressed now the air density is only a function of the radial distance from the center of the Earth. However, the Earth is an oblate spheroid and hence produces a latitude effect to the atmospheric properties. This atmospheric oblateness and aforementioned solar activity cause the main distortions from spherical symmetry. More complex models of the atmosphere have been devised to account for these variational effects. See Reference 4.

Satellite Velocity. The component V in the atmospheric drag equation represents the satellite's velocity relative to the atmosphere. With \bar{v}_a being the velocity vector of the air and \bar{v} the satellite's velocity vector (both with respect

to an Earth fixed coordinate frame)

$$\bar{V} = \bar{v} - \bar{V}_a \quad (29)$$

Squaring Eq (29) yields

$$V^2 = v^2 + V_a^2 - 2 v V_a \cos \gamma \quad (30)$$

where γ is the angle between \bar{V}_a and \bar{v} .

Let ω represent the atmospheric rotation rate. This angular velocity is assumed to be uniform about Earth's North-South axis (27:275). Thus

$$V_a = r \omega \cos \phi \quad (31)$$

where

r \equiv distance from Earth's center

ϕ \equiv geocentric latitude

For small eccentricities, a satellite travels nearly horizontal through the atmosphere (and exactly horizontal for circular orbits). A very small error ($< 1\%$) results if the angle γ is taken as angle γ^* , the angle between \bar{V}_a and the horizontal component \bar{v}_H of \bar{v} (15:23). See Figure 4.

Examining spherical triangle SNL

$$\cos \gamma^* \cos \phi = \cos i \quad (32)$$

Eq (31), with $\gamma \approx \gamma^*$, becomes

$$V_a \cos \gamma = r \omega \cos i \quad (33)$$

Substituting this result into Eq (30) produces

$$V^2 = v^2 [1 - (r\omega/v) \cos i]^2 + r^2 \omega^2 (\cos^2 \phi - \cos^2 i) \quad (34)$$

Further assumptions to Eq (34) can be made due to the variable and unknown rotation of the Earth's atmosphere.

First, the $r^2 \omega^2$ term can be neglected due to $r^2 \omega^2 < .005 v^2$

The quantity F represents the effect of atmospheric rotation on the drag force. Assuming ω is equal to Earth's rotation rate, F will normally lie between 0.9 and 1.1 and, although the effect of atmospheric rotation on drag is slight, it is not inconsequential (15:25).

Coefficient of Drag. The drag coefficient C_d is an important element in the aerodynamic drag equation. While a more accurate value of the total aerodynamic force can be determined using a differential force equation it is more convenient to use the drag coefficient in the orbital analysis (19:9). When working with a coefficient of drag several assumptions must be made concerning the atmospheric molecules (15:14-15):

- 1) The satellite is considered to be stationary with the air molecules flowing past.
- 2) The molecules are assumed to impinge on the satellite, be retained temporarily on its surface, and then re-emitted.
- 3) The collisions between incident and re-emitted molecules are neglected.

Several factors come into play in calculating the drag coefficient. The first parameter to consider is the flow regime through which the satellite moves. This flow type is determined by the Knudsen number, defined as the ratio of mean free path of atmospheric molecules to the characteristic linear dimension of the satellite (11:184). Two hundred

kilometers above the Earth the ordinary continuum flow of conventional aerodynamics no longer applies because of the extremely low air density (15:14). This region is called free molecular flow and has a Knudsen number of 10 or greater (11:184). When a satellite is in this flow regime its drag coefficient is dependent on the molecular speed ratio. This is the ratio of satellite speed to most probable molecular speed. For altitudes below 700 km this speed ratio always exceeds 5. This implies that the random thermal motion of the atmospheric molecules can be ignored; i.e., the flow is hyperthermal (3:931).

Another factor to the drag force is the mechanism of molecular reflection. The energy exchange between the atmosphere molecules and the satellite is dependent on both the direction of the reflected molecules and their speed. It is assumed the air molecules that impinge on the satellite's surface do not reflect specularly but instead attach themselves to the outer layer of the surface for a period of time before being re-emitted. During this period the molecules 'forget' their original direction of motion and are re-emitted diffusely. This diffuse reflection is strongly contingent upon the nature of the satellite's surface and its structure (3:931).

The speed of the re-emitted molecules is determined by their kinetic temperature. During the period of attachment the molecules also 'forget' their original temperatures. By how much they 'forget' is uncertain (15:15) and leads to

the accommodation coefficient, defined as

$$\alpha = \frac{T_i - T_r}{T_i - T_s} \quad (38)$$

where

- T_i = original molecular temperature
- T_r = re-emitted molecular temperature
- T_s = satellite surface temperature

Theoretical values of the accommodation coefficient are very difficult to determine. Many assumptions must be made concerning the gas molecules and their interaction with the satellite's outer surface. It is suggested that low values of the coefficient are appropriate (3:931,934). This implies higher drag coefficients. Reference 15, on the other hand, assumes from "conflicting and rather unsatisfactory" experimental results that the accommodation coefficient is nearly 1.0 but admits this assumption may be wrong (15:15).

Reference 3 presents a graph of drag coefficients versus accommodation coefficients for a circular cylinder with its axis perpendicular to the direction of motion. Hyperthermal free molecular flow and a T_s/T_i ratio of 0.006 are both assumed (3:939). See Figure 5. The upper line is a plot of $C_d = 2(1 + \pi/6 r)$ where diffuse re-emission is assumed. The term r here is a ratio of the speed of a re-emitted molecule V_r to the speed of an incident molecule V_i and is related to α by

$$r = \frac{V_r}{V_i} = [1 + \alpha (T_s/T_i - 1)]^{1/2} \quad (39)$$

The ratio T_s/T_i is very small so r can be approximated by

$$r = [1 - \alpha]^{1/2} \quad (40)$$

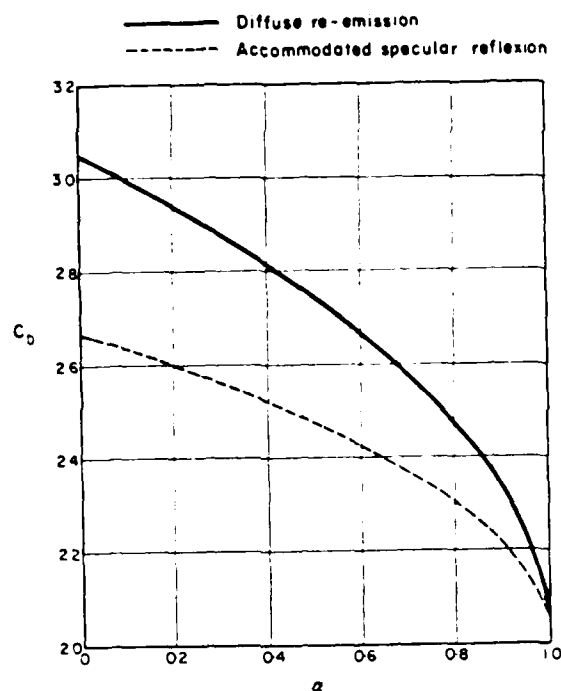


Figure 5. Circular Cylinder Drag Coefficient

The last factor to consider in determining the drag coefficient is the satellite's dynamics and orientation to the atmospheric flow. For a cylinder tumbling end over end

$$C_d = 2 \left[1 + \frac{\pi^2 (1+d)}{6 (4l+d)} r \right] \quad (41)$$

where

l = cylinder length

d = cylinder diameter

This equation for C_d produces similar results for various values of l/d (3:940).

Satellite Area. The projected area normal to the free molecular flow of Earth's upper atmosphere also affects the drag force experienced by the satellite. The size of this area depends upon the orientation of the satellite as it orbits the Earth. For a cylindrical shaped body in a gravity gradient stabilized position the projected area is simply $l \times d$, where l is the length and d is the diameter. At the other extreme, for a cylinder pointed into the air flow, the projected area is $\pi d^2/4$.

However, a satellite might not remain in these constant area positions relative to the flow. The system's orbital dynamics can also alter the size of the projected area. Reference 29, in a comparison of space environment torques, concludes that below 200 nm (≈ 370 km) aerodynamic torques dominate a satellite's dynamics whereas above 300 nm (≈ 555 km) the gravity gradient torques are the major influences. Between these altitudes both space torques can interact to cause an unstable disturbance in the satellite's orientation (18:2200). An uncontrolled satellite, with any initial rotational motion, will soon begin spinning about its axis of greatest moment of inertia. This action is caused by these relatively small external torques (15:16).

With its maximum moment of inertia axis being its transverse axis, the cylinder (with $l/d > 2$) could assume an orientation where its spin axis is aligned with the air flow (15:16). This would be its "aeroplane propeller" motion and again the projected area is $l \times d$. Conversely, the

cylinder could have its spin axis pointing 90 degrees to the air flow, tumbling end-over-end. The mean cross-sectional area in this case is $2/\pi (ld + 1/4 \pi d^2)$. Of course other spin axis directions are also possible and the projected area would lie between these two extreme values. Reference 15 presents an expression for the mean of these values as

$$A = ld (0.818 + 0.25 d/l) \quad (42)$$

The two perturbations discussed in this chapter are the major disturbances affecting a satellite's orbit about the Earth. Each has its own unique impact but cannot be considered separately in an orbital analysis of an External Tank. The results of this ET study will show the coupling effect between them that alters the satellite's orbital decay rate.

IV. Program Implementation

This chapter outlines the approach used by the Artificial Satellite Analysis Program to model the Earth's gravitational field and atmosphere. The constants and variables that describe the primary and its gravitational field, the atmosphere, and the External Tank and its orbit are also included.

Earth, as the primary in this investigation, is defined by the following parameters (16:II-14):

- 1) μ : $3.986006 \times 10^5 \text{ km}^3/\text{sec}^2$
- 2) R_e : 6378.14 km
- 3) ω_e : $0.4178074216 \times 10^{-2} \text{ deg/sec}$
- 4) e_e : 0.08199

ASAP incorporates Earth's gravitational field through use of the geopotential expansion series Eq (15). The ET's position in its orbit is correlated with the associated radius, latitude and longitude of the geopotential and the disturbing acceleration is calculated. The values for the spherical harmonic coefficients C_{lm} and S_{lm} of Eq (15) that define Earth's mass distribution come from Table I.

For perturbations caused by a planet's atmosphere ASAP uses a simple exponential density model as expressed by Eq (22). Reference 20 is the source of Earth's atmospheric density and scale height values at various reference

altitudes. This is a static atmosphere model (no time dependence) that attempts to describe 'average' atmospheric properties which represent a mean value of the diurnal, seasonal and other solar-caused variations detailed in the previous chapter. ASAP also assumes the atmosphere is rotating at the same rate the Earth itself rotates and includes the atmospheric oblateness in its calculations.

The External Tank is the main structural element of the Space Transportation System, supporting both the Orbiter and the two Solid Rocket Boosters (See Figure 6). The tank consists of three main components: the LO_2 tank, the intertank and the LH_2 tank. These ET components are

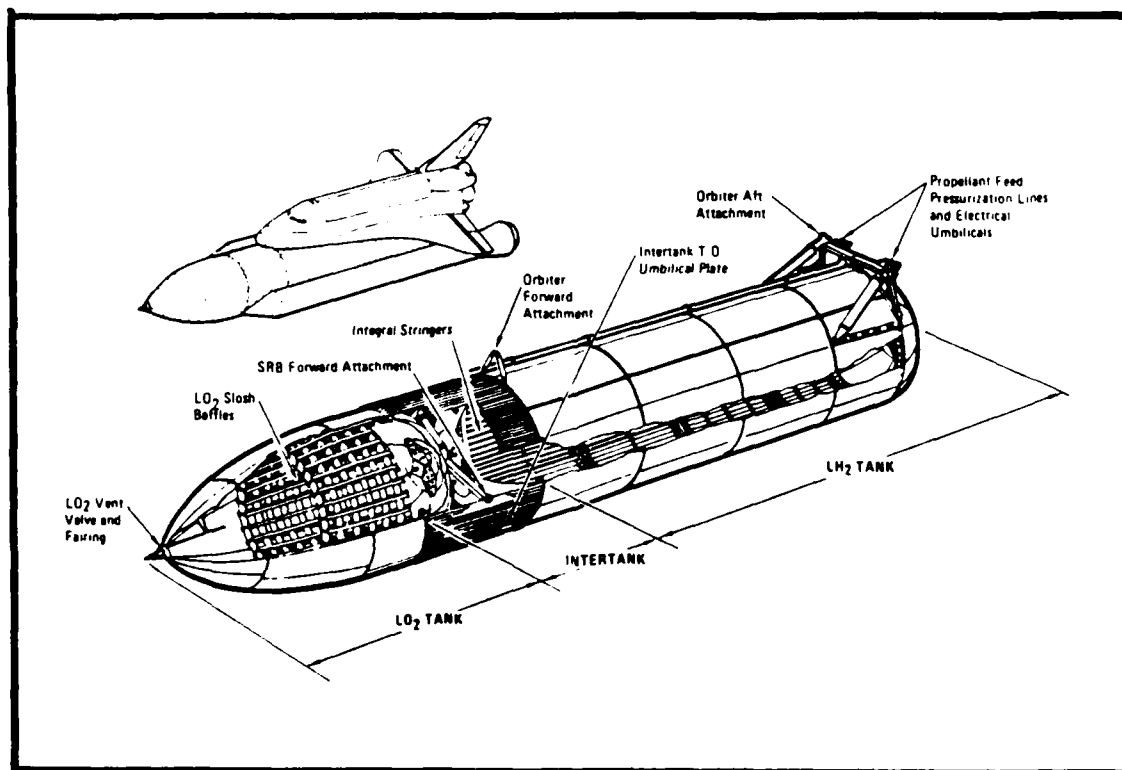


Figure 6. STS External Tank

manufactured from an aluminum alloy and, after assembly, the unit is coated with a 1 to 1-1/2 inch layer of spray-on foam insulation (8:II-1). The following External Tank numbers are used for the orbital analysis:

- 1) Weight : 33503 kg
- 2) Area (normal to flow) : 353 m²
- 3) Cd : 2.4

The tank weight figure comes from Reference 10 and represents an inert weight. It is assumed that most of the residual fuel at normal jettison altitude would be used to boost the Orbiter and ET into a higher orbit.

According to Reference 8, the ET, once left in orbit, will assume a gravity gradient orientation where the longitudinal axis of the tank points toward the center of the Earth. Reference 17 states that the gravity gradient torque on an External Tank orbiting between 400 and 500 km would dominate all other environmental torques, including moments caused by aerodynamic forces. This situation will expose the greatest amount of tank area to the oncoming air molecules. Of course in reality, the Shuttle would jettison the ET with its nose pointed into the atmospheric flow and there would be a certain amount of time before the tank stabilized into the gravity gradient position. In this case the mean projected area normal to the flow would be less than 353 m² resulting in less altitude loss over the 90-day period. However, for the purposes of this thesis, the worst case for the projected

area will be considered where the External Tank is dropped off directly into a gravity gradient position. This ET area is calculated from dimensions given in Reference 26.

For cylindrical shaped satellites, drag coefficients derived in References 3,9,11,15 and 22 range in value from 2.0 to 3.0. Modeling the External Tank as a cylinder, a C_d of 2.4 is used as a representative figure.

The classical Keplerian elements ($a, e, i, \Omega, \omega, M$) are used to define the initial starting conditions of the orbiting External Tank. During preliminary orbit investigations various values of Ω, ω and M were evaluated and found to have no discernable effect on the 90-day altitude loss rate. For this reason, during all subsequent test runs, these three elements are set to zero for the initial orbit condition.

V. Results

The results of this thesis are discussed in two sections. The first section details the search for the lowest possible altitude for the defined External Tank parking orbit: Maximum 25 km altitude loss over 90 days. The orbital elements of this minimum altitude orbit are then explored. The second section investigates various aspects of the orbit, gravitational field, atmosphere and ET characteristics to determine their effect on the magnitude of altitude loss. An introductory section is needed however to define 'altitude loss' as used in this thesis.

Altitude Loss Definition

Figure 7 is a plot of the daily fluctuations in geocentric altitude of an orbiting External Tank perturbed by both a gravity field and atmospheric drag. These fluctuations do not lead to an easy statement of the amount of altitude lost by the ET over the 90-day period. However, a regression function is used to perform a linear least squares fit to the data. See Figure 8. The program calculates the slope of this line which represents the mean altitude loss rate. It is therefore very convenient to define the altitude loss in kilometers as:

$$90\text{-Day Altitude Loss} = \text{Line Slope (km/day)} \times 90 \text{ (days)}$$

GEOCENTRIC ALTITUDE FLUCTUATIONS

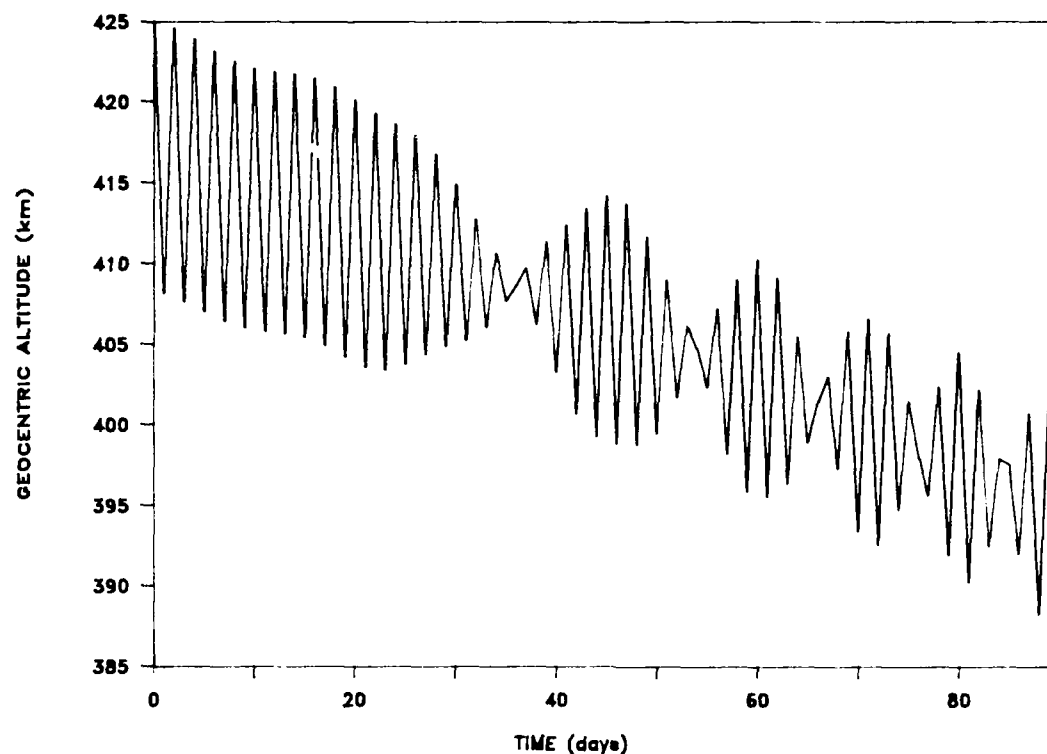


Figure 7. Geocentric Altitude Fluctuations

Minimum Parking Orbit Altitude

To perform this phase of the External Tank study initial conditions of 28° inclination and zero eccentricity were used. A 3x3 gravitational field and a simple atmosphere model were integrated into this analysis. The search for the minimum altitude began at 500 km and progressed downward at 25 km increments. Computer test runs were conducted until the parking orbit constraint had been violated. Results of this investigation are reported in Table II. Due to the exponen-

REGRESSION OF GEOCENTRIC ALTITUDE DATA

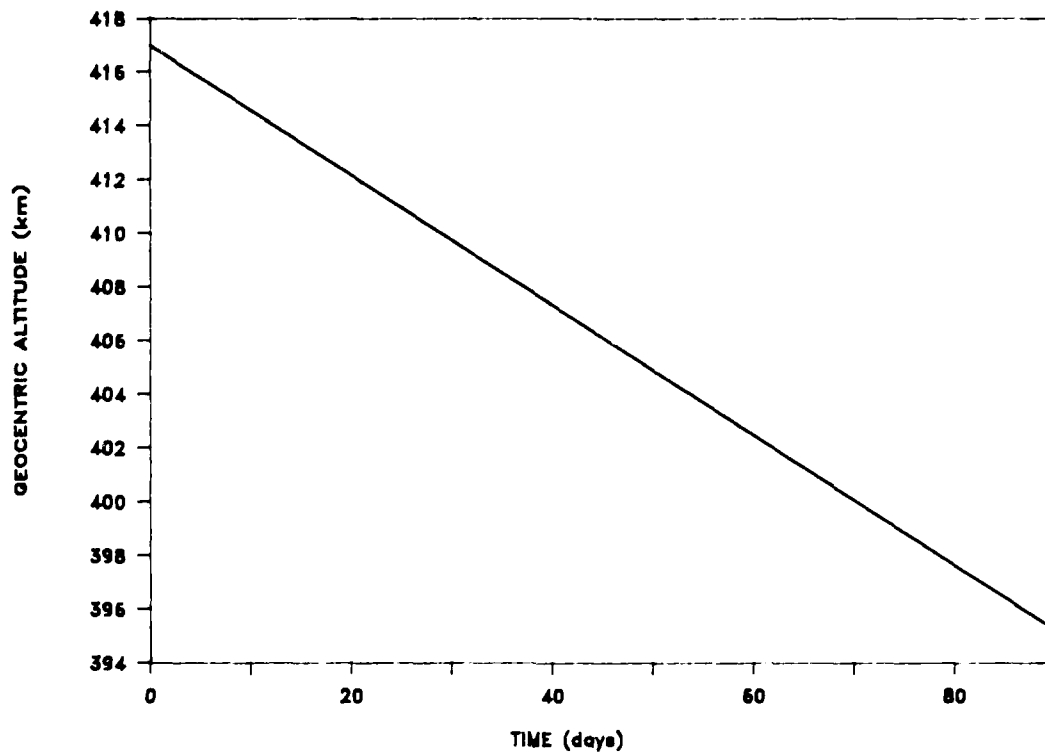


Figure 8. Linear Regression to Geocentric Altitude Data

tial nature of the atmospheric density, there is a substantial increase in the altitude loss rate as the initial altitude of the ET orbit decreases. The altitude of 425 km meets the established parking orbit criteria.

Time History of the Orbital Elements

Using 425 km as the initial altitude for the External Tank orbit, the orbital elements were investigated for a period of 90 days. Due to the fluctuations in the elements,

TABLE II
90-Day Altitude Loss for Initial ET Altitudes

<u>Initial Orbit Altitude (km)</u>	<u>90-Day Altitude Loss (km)</u>
500	5.5
475	8.4
450	13.2
425	21.8
400	38.2

a curve fitting program was adapted from Reference 7. This technique suppresses the short term variations in the orbital elements and allows the long period behavior to be seen. The program calculates the coefficients to 1st, 2nd and 3rd order polynomials and determines which order equation produces the best fit to the data. These polynomials developed for the orbital elements represent a convenient method to calculate the External Tank's orbit at some future time t within the 90-day period studied. Figures 9 through 13 are plots of the daily variation in the orbital parameters and the associated long period trend line.

Semi-Major Axis (Figure 9). The semi-major axis of this External Tank parking orbit contracts by 21.4 km ($\sim 0.3\%$) during the 90-day period. The long term trend line is a 2nd order polynomial:

$$a = 6801.2279327 - 0.2122813 t - 0.0003232 t^2 \quad (43)$$

Polynomials generated for other initial altitudes show that a

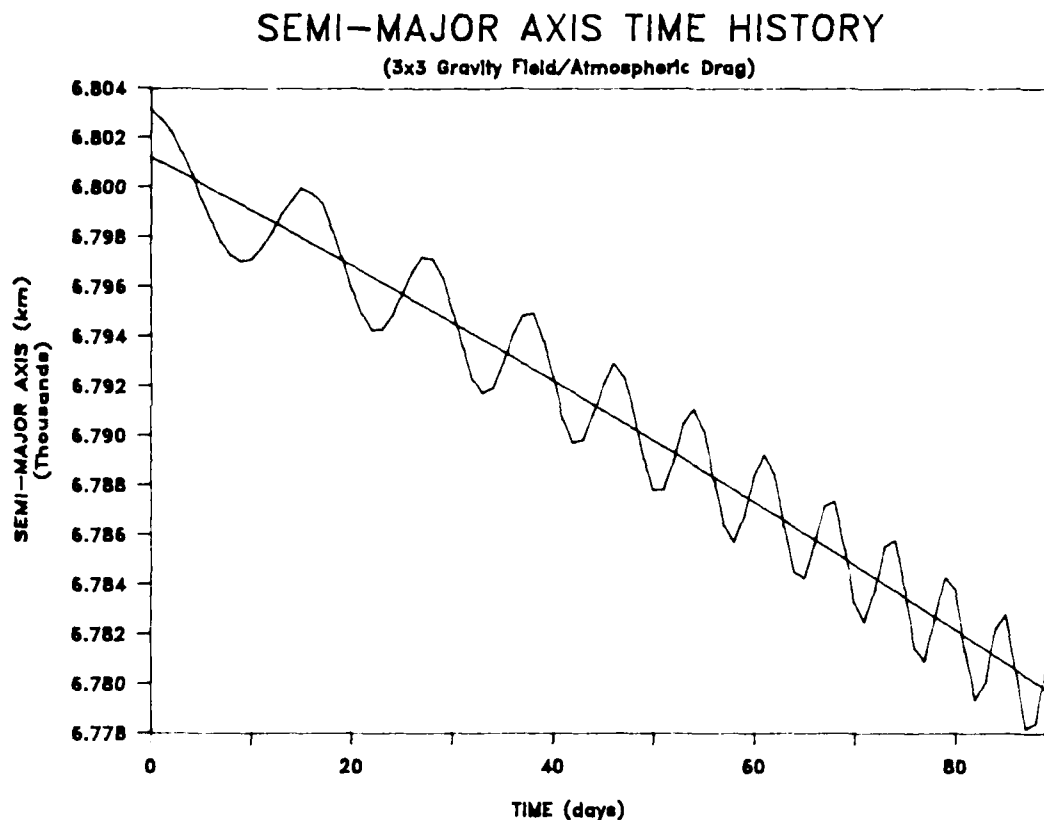


Figure 9. Semi-Major Axis Time History

1st order equation is adequate for 500 and 475 km but starting at 450 km a 2nd order polynomial is required for the best fit to the semi-major axis data.

Eccentricity (Figure 10). Although the External Tank was placed in a circular orbit ($e = 0$) for this investigation, the value of this orbit's eccentricity did not remain at zero. This variation in eccentricity is produced by the gravitational perturbations. The best fit polynomial is

1st order

$$e = 0.0012661 + 0.0000010 t \quad (44)$$

and indicates a slight increase in the eccentricity over the 90-day time frame. While the overall effect of the atmosphere is to circularize a satellite's orbit, i.e., drive the eccentricity to zero, over a given time period the mean value of the eccentricity may show a slight increase as shown by the long period trend line.

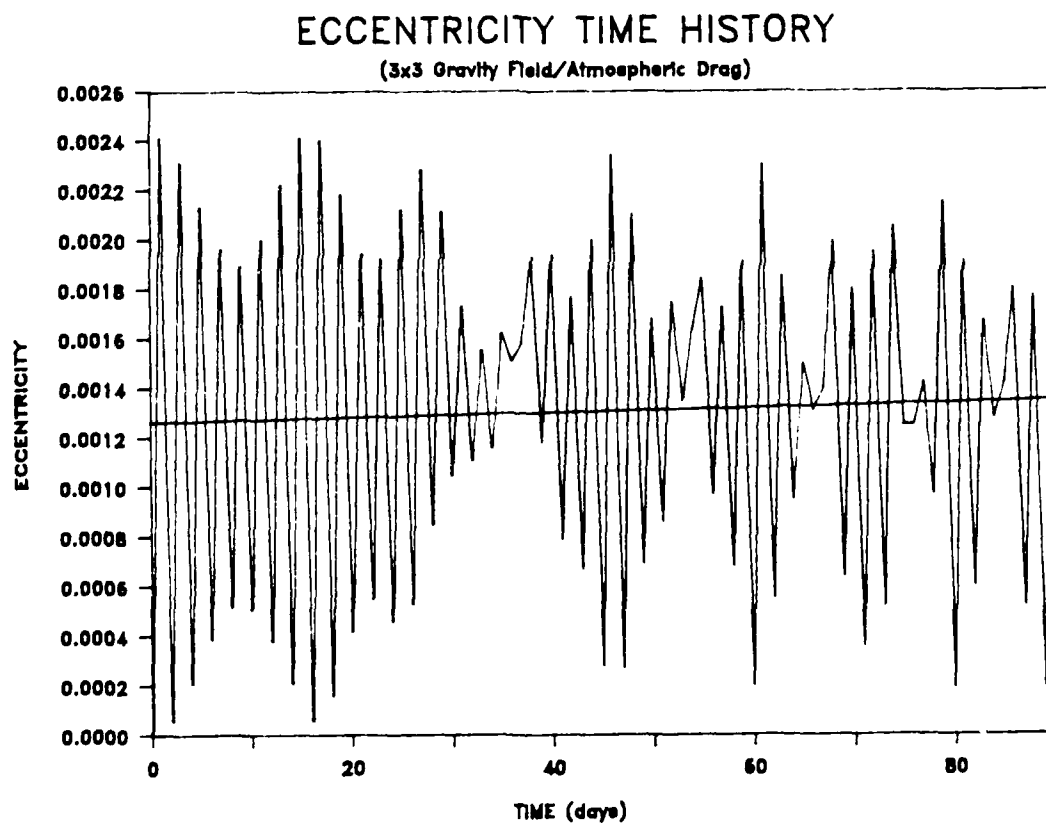


Figure 10. Eccentricity Time History

Inclination (Figure 11). This figure shows the variations in the ET's orbit inclination over the 90-day period. The mean value, as described by

$$i = 27.9844744 - 0.0000193 t \quad (45)$$

displays a minuscule decrease. As with the eccentricity, this decrease in the inclination is valid for the 90-day period only. The perturbations as modelled have no secular effects on an orbit's inclination (15:8).

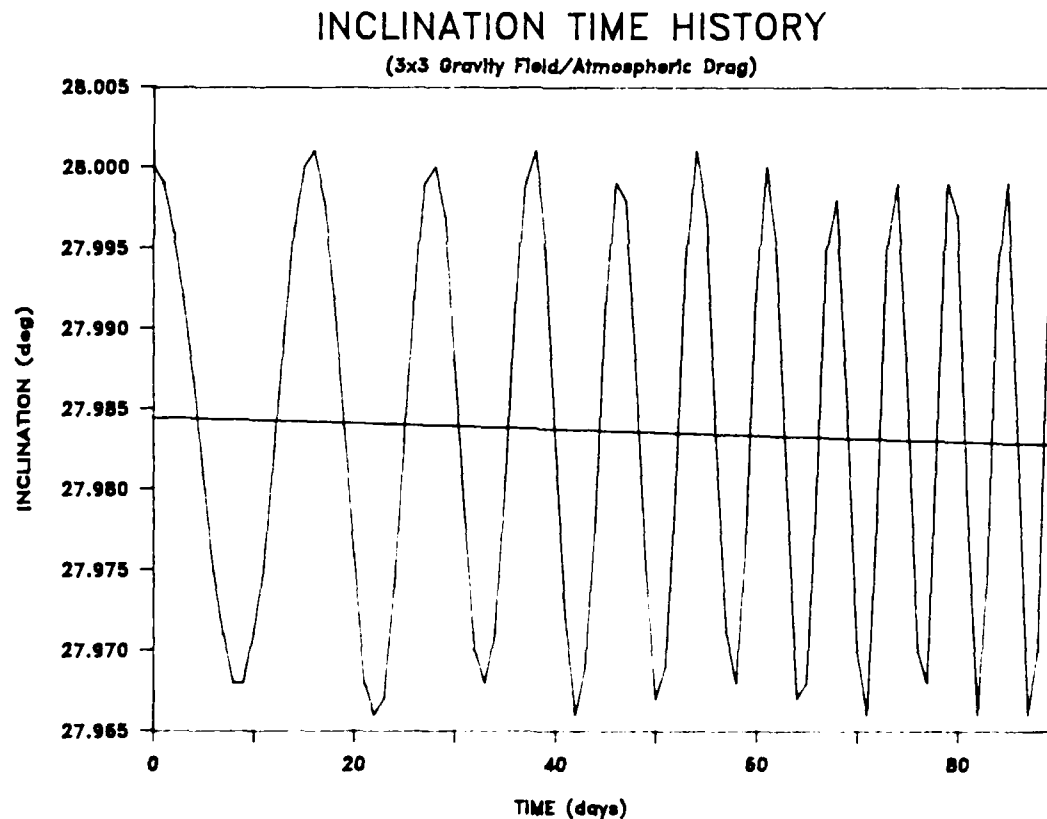


Figure 11. Inclination Time History

Longitude of Ascending Node (Figure 12). The best fit polynomial for this orbital element

$$\Omega = 360.1578150 - 7.0659969 t \quad (46)$$

exactly matches the data generated by ASAP. This graph has the node initialized at 360° and indicates the External Tank's orbital plane rotates about Earth's polar axis approximately once every 50 days or about 7° per day. This effect on Ω is caused by gravitational perturbations (15:7-8).

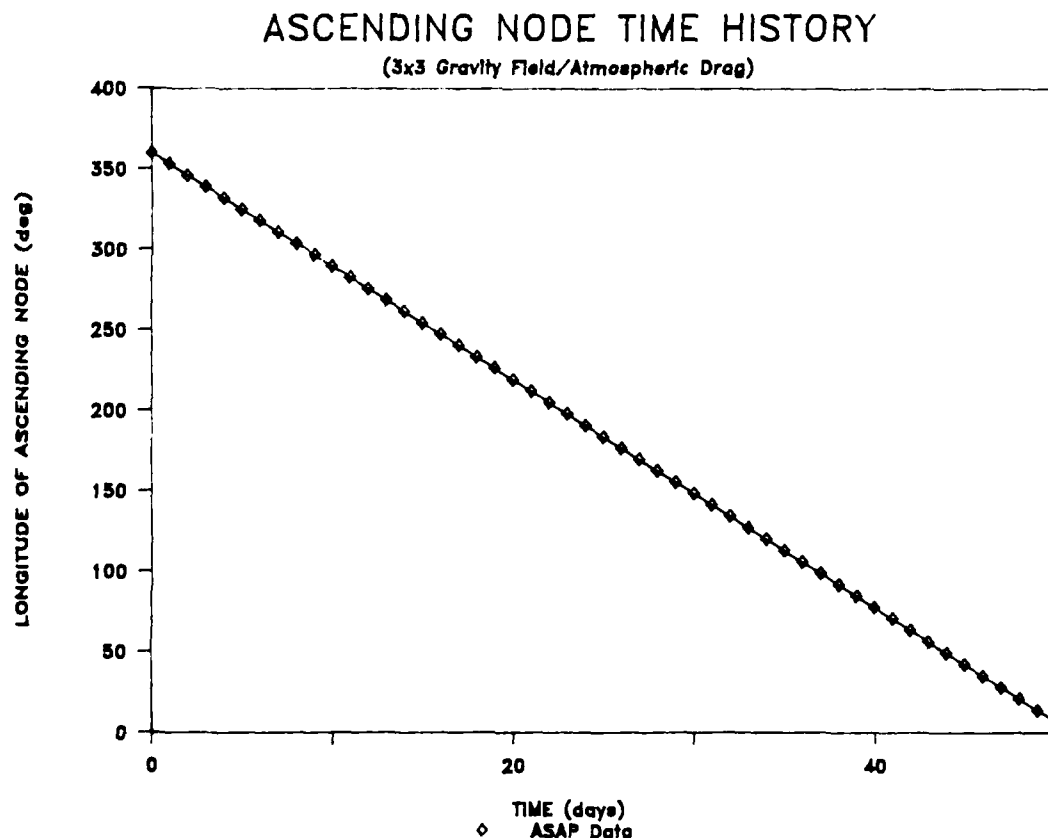


Figure 12. Longitude of Ascending Node Time History

Geocentric Altitude (Figure 13). The daily variation in the geocentric altitude of the External Tank is the result of the varying force of attraction on the tank caused by Earth's gravity field. The best fit polynomial is 1st order

$$\text{Geo. Alt.} = 417.1935674 - 0.2459279 t \quad (47)$$

and shows an altitude loss rate of about 0.25 km per day.

Orbital element polynomials for other altitudes are contained in Appendix B. The next section of the results will discuss the different influences on the External Tank altitude loss rate.

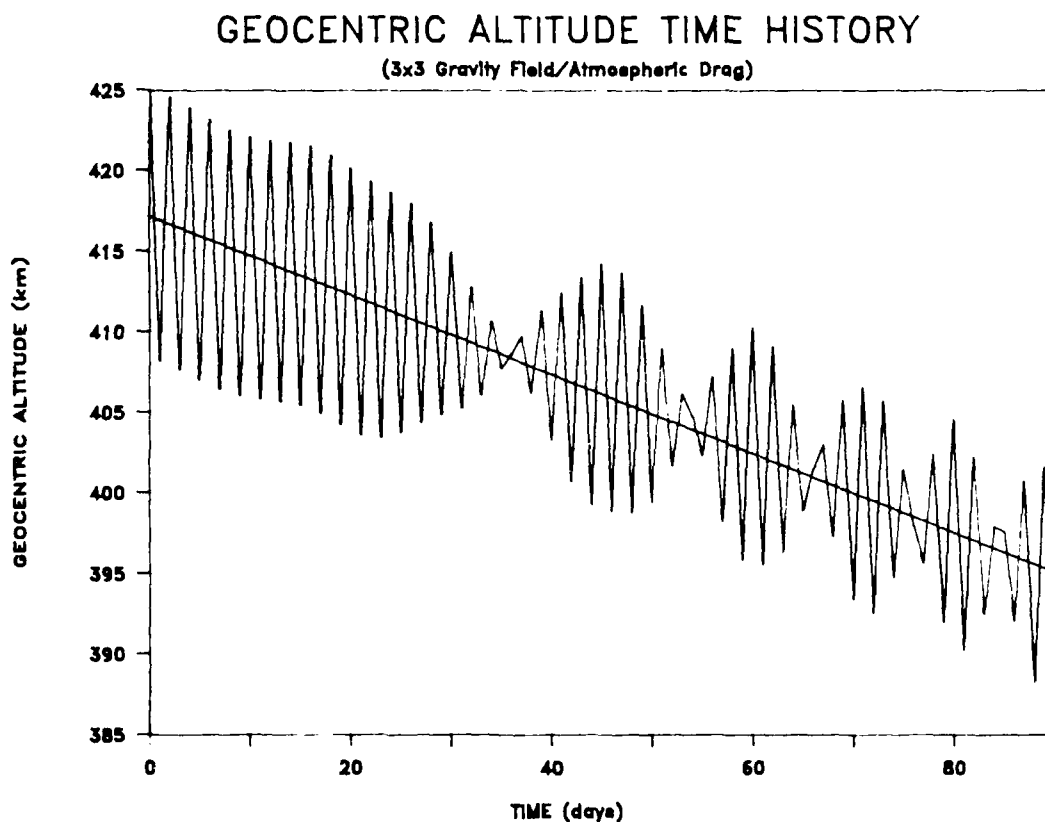


Figure 13. Geocentric Altitude Time History

Initial Altitude Effects

Ninety-day altitude loss data from the parking orbit investigation in Section I was used to produce Figure 14. At 500 km the upper atmospheric density is extremely low and the External Tank loses very little altitude during the 90 days. However, at lower altitudes the atmospheric drag becomes more of a factor and shrinks the ET's orbit considerably.

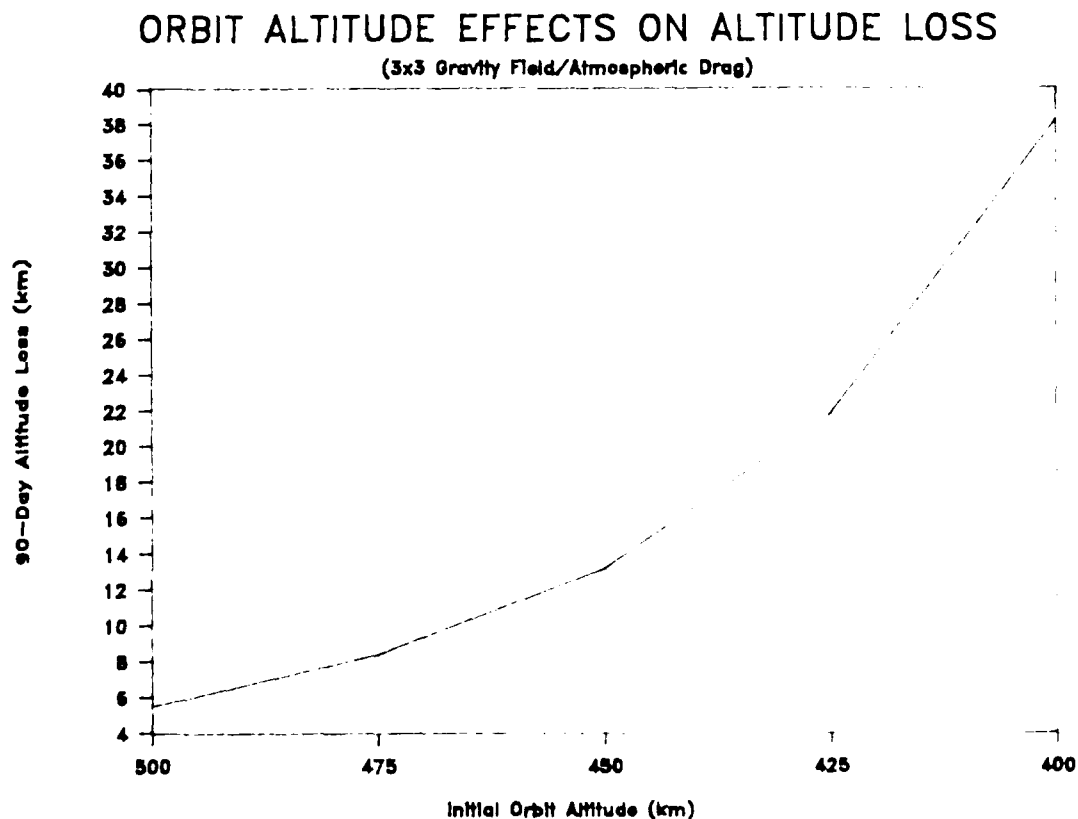


Figure 14. Initial Altitude Effects on Orbit D Day

Orbital Element Effects: Inclination and Eccentricity

Both these investigations were conducted using a 3x3 gravitational field and a simple atmosphere model. The initial altitude of the External Tank orbit was 425 km.

For the inclination study test runs were made at 18, 23, 28, 33, and 38 degrees with zero initial eccentricity in each case. Figure 15 indicates the slight increase in the 90-day altitude loss as the orbit inclination is decreased. This effect is due to the oblateness of the modelled atmosphere where, for a given altitude, the air is slightly thicker at the equator than at the poles.

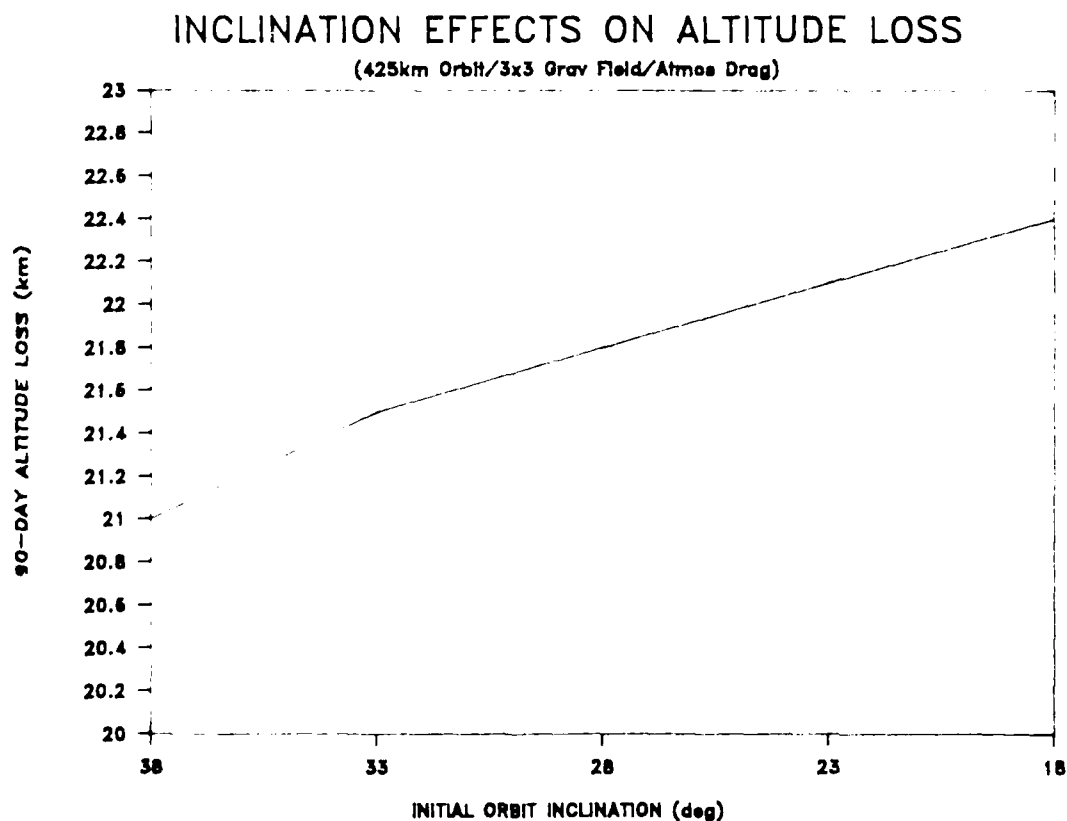


Figure 15. Inclination Effects on Orbit Decay

For the next study test cases were run with eccentricity values of 0.0, 0.005, 0.0075 and 0.01 with an initial inclination of 28° in each case. As seen from Figure 16, by increasing the initial eccentricity of the ET's orbit, the 90-day altitude loss increases. The explanation of this effect is found by looking at the variation in the geocentric altitude which, in turn, determines the atmospheric density. For near zero eccentricity orbits, the value of geocentric altitude will vary as was shown in the first section of the results. However, as the eccentricity is increased, it is

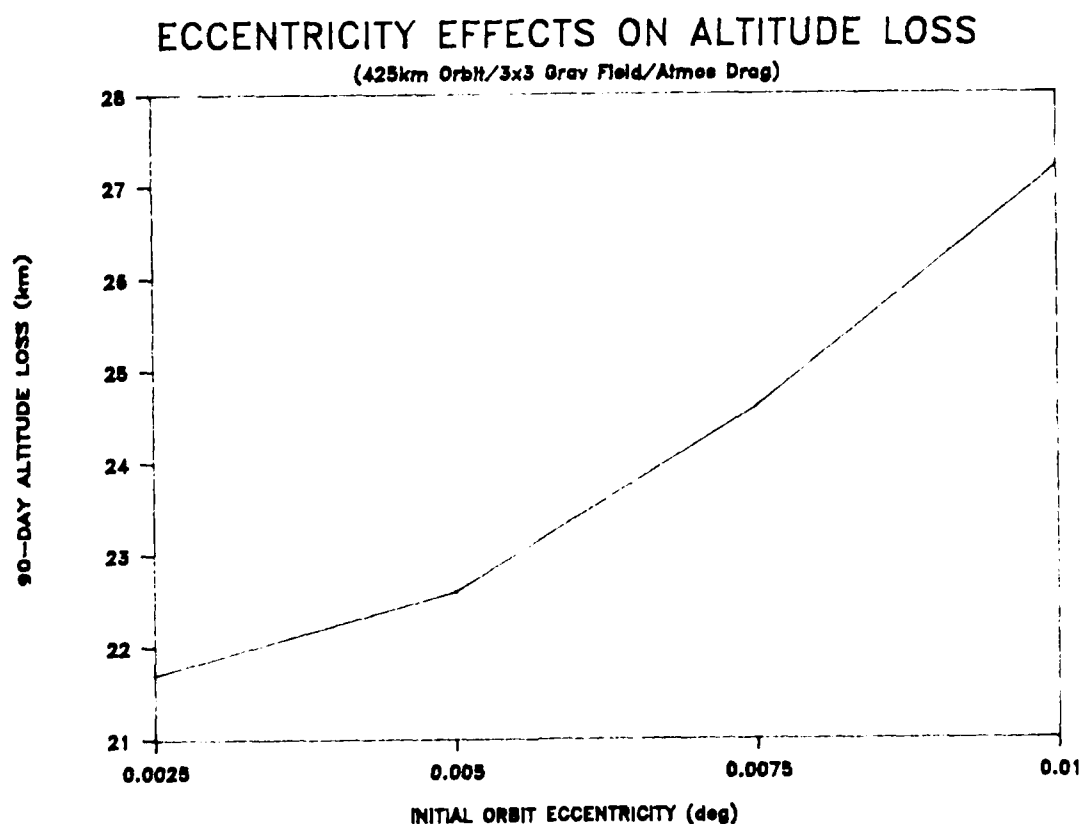


Figure 16. Eccentricity Effects on Orbit Decay

found that the fluctuations in geocentric altitude become larger. This results in the External Tank being exposed to higher values of air density in addition to having a higher orbital velocity at the lower extremes. These two factors result in a greater drag force as expressed by Eq (20).

Gravitational Field Effects

In the first part of this study the External Tank was put in an orbit with initial conditions of 28° inclination and zero eccentricity with computer runs made at initial altitudes of 425 and 500 km. For each altitude 90-day orbits were calculated using a simple atmosphere model with and without a 3x3 gravity field. Table II details the coupling effect between these two orbit perturbations. Due to the varying gravitational attraction of a 3x3 field, the ET finds itself at times pulled into a lower than normal orbit thereby experiencing greater atmospheric drag forces. The overall effect of a complex geopotential, combined with an atmosphere, is a higher rate of altitude loss.

TABLE III
Air Drag/Gravity Field Coupling Effects

<u>Altitude (km)</u>	<u>90-Day Altitude Loss (km)</u>	
	<u>Air Drag</u>	<u>Air Drag + 3x3 Grav Field</u>
500	4.8	5.5
425	18.3	21.8

The next investigation into the gravitational field effects on altitude loss concerns the degree of complexity needed for acceptable results. Using an initial External Tank orbit of 425 km altitude, 28° inclination and zero eccentricity, test cases were run with a simple atmosphere and models of the following geopotential fields: 2x0, 2x2, 3x1, 3x3. In all four cases the 90-day altitude loss was 21.8 km. The 2x0 field models the oblate shape of the Earth and is the dominant gravitational perturbation.

Atmospheric Density Effects

The simple exponential atmosphere model is one of the major assumptions made in this orbital analysis of an External Tank. This static model leaves out the dynamic characteristics of Earth's atmosphere as discussed in Chapter III. All the fluctuations in the atmospheric properties are averaged to produce a mean density. However, over any designated time period, the value of this mean density at any given altitude could be much higher than that cited by Reference 20. Subsequently, a series of computer runs were done to study the effects of increased atmospheric density on an External Tank's orbit. Density numbers, with associated scale height values, were taken from Reference 12 covering a low-density to a medium-density atmosphere. An ET orbit of 425 km altitude, 28° inclination and zero eccentricity

formed the basis for studying the 90-day altitude loss. As was the case when the various starting altitudes were examined, a higher mean value of air density will cause the ET's altitude to decrease markedly. See Figure 17.

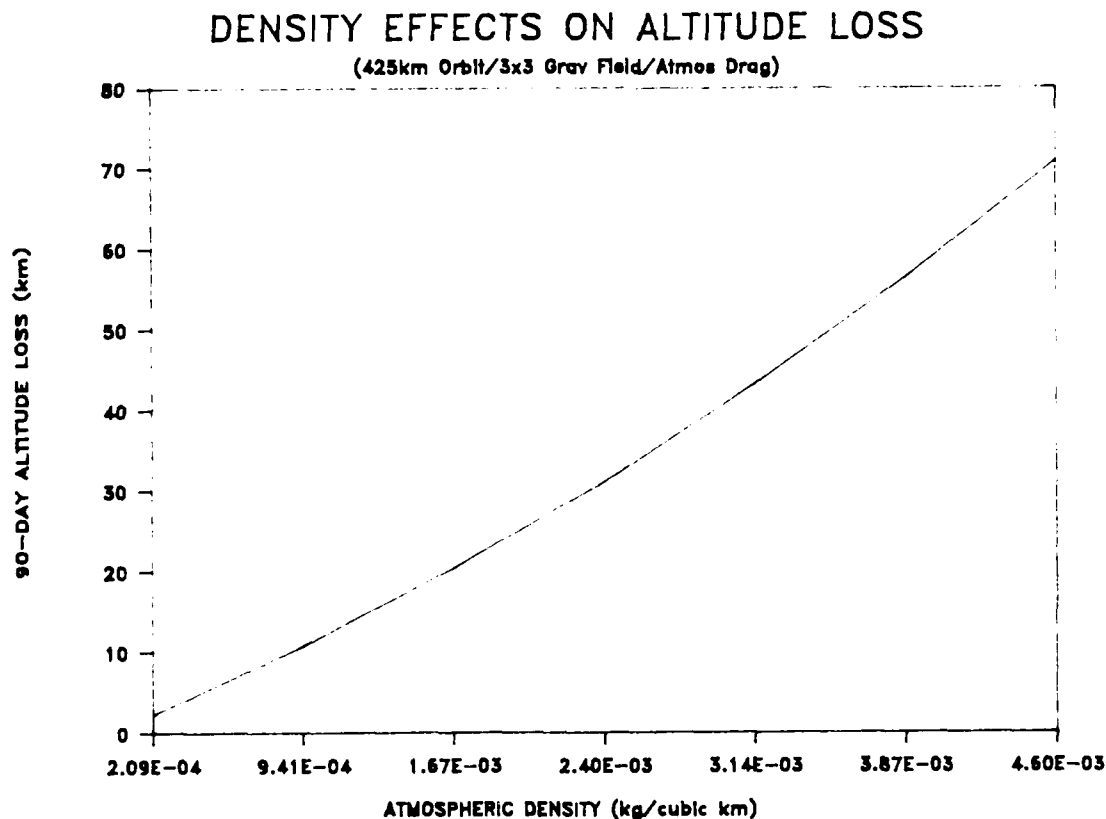


Figure 17. Atmospheric Density Effects on Orbit Decay

External Tank Characteristics Effects

The values used in this thesis for the External Tank's projected area to the air flow and it's drag coefficient are valid assumptions but by no means certainties. As was discussed in Chapter III a combination of gravitaional and

aerodynamic forces can produce different orientations of an orbiting spacecraft which, in turn, will affect the magnitude of the projected area and drag coefficient. With this in mind a study was done using the ballistic coefficient as a parameter to vary. From Eq (38)

$$B = \frac{C_d A}{2m} \quad (48)$$

For an ET kept with its front end into the air flow, the projected area would be 55 m^2 . Conversely, the gravity gradient profile has an approximate area of 353 m^2 .

References 23 and 30 give higher C_d values for various orientations of a cylindrical satellite so a C_d range of 2 to 5 is used, along with an ET mass of 33503 kg, to calculate a minimum and maximum ballistic coefficient. The minimum would be

$$B_{\min} = \frac{(2) (55)}{(2) (33503)} = 1.64 \times 10^{-3} \text{ m}^2/\text{kg}$$

and the maximum

$$B_{\max} = \frac{(5) (353)}{(2) (33503)} = 2.63 \times 10^{-2} \text{ m}^2/\text{kg}$$

Computer runs were done using ballistic coefficients of 1.64×10^{-3} , 9.86×10^{-3} , 1.81×10^{-2} and $2.63 \times 10^{-2} \text{ m}^2/\text{kg}$ convolved with initial altitudes of 400, 425, 450 and 475 km, and with nominal values of 28° inclination and zero eccentricity. This convolution of ballistic coefficients and starting altitudes produced 16 values of 90-day altitude loss. To develop an idea of the External Tank characteristics and their effect on the loss rate a 3-dimensional plot was

formed the basis for studying the 90-day altitude loss. As was the case when the various starting altitudes were examined, a higher mean value of air density will cause the ET's altitude to decrease markedly. See Figure 17.

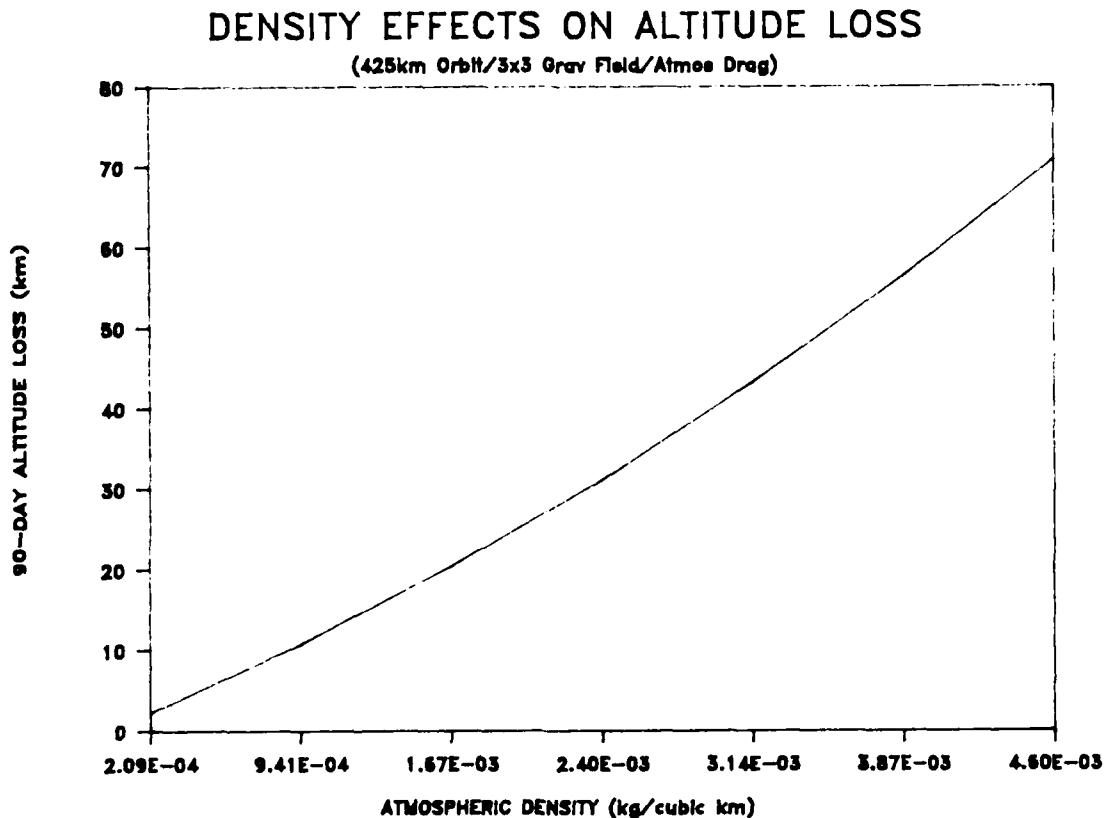


Figure 17. Atmospheric Density Effects on Orbit Decay

External Tank Characteristics Effects

The values used in this thesis for the External Tank's projected area to the air flow and it's drag coefficient are valid assumptions but by no means certainties. As was discussed in Chapter III a combination of gravitaional and

accomplished (See Figure 18. Note: Due to the graphics program operation the ballistic coefficients labelled on this plot should be multiplied by 2×10^{-4}).

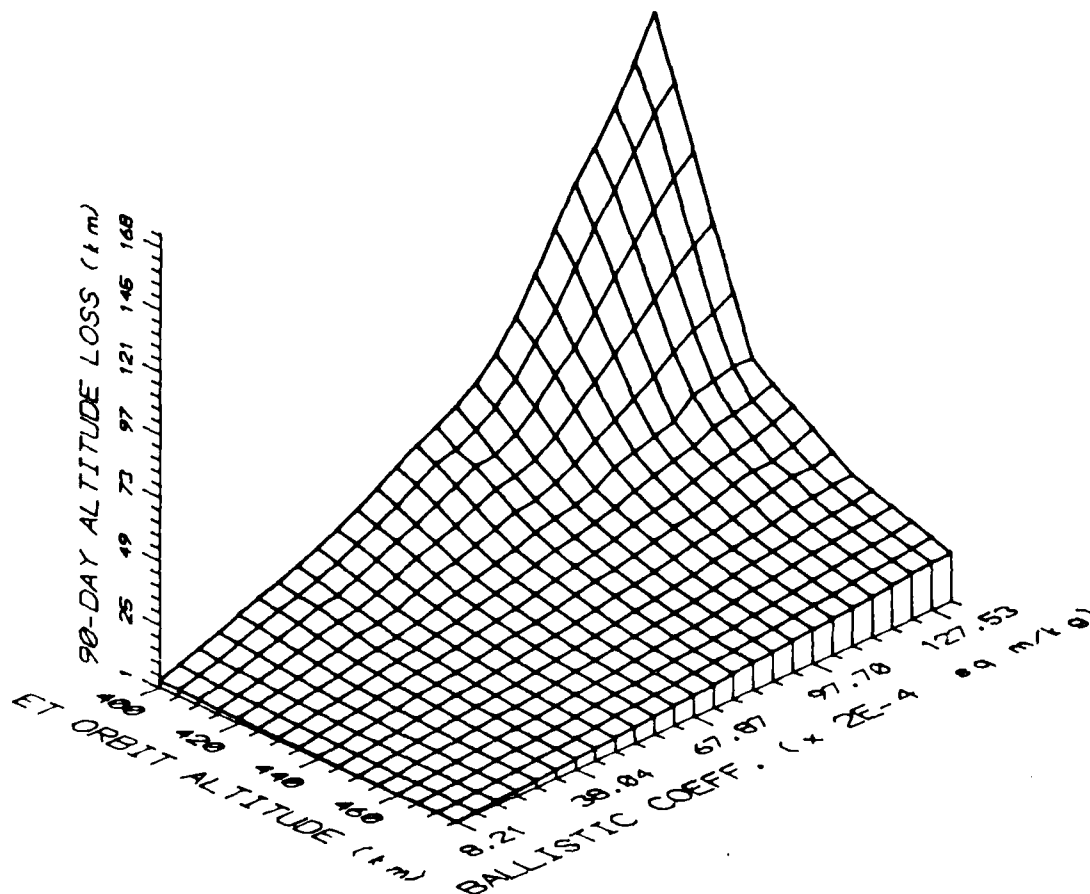


Figure 18. 3-D Graph of 90-Day Altitude Loss

Figure 19 is a contour plot of the same data giving a clearer picture of the 90-day altitude loss for various combinations of ballistic coefficient and initial External Tank orbit altitude.

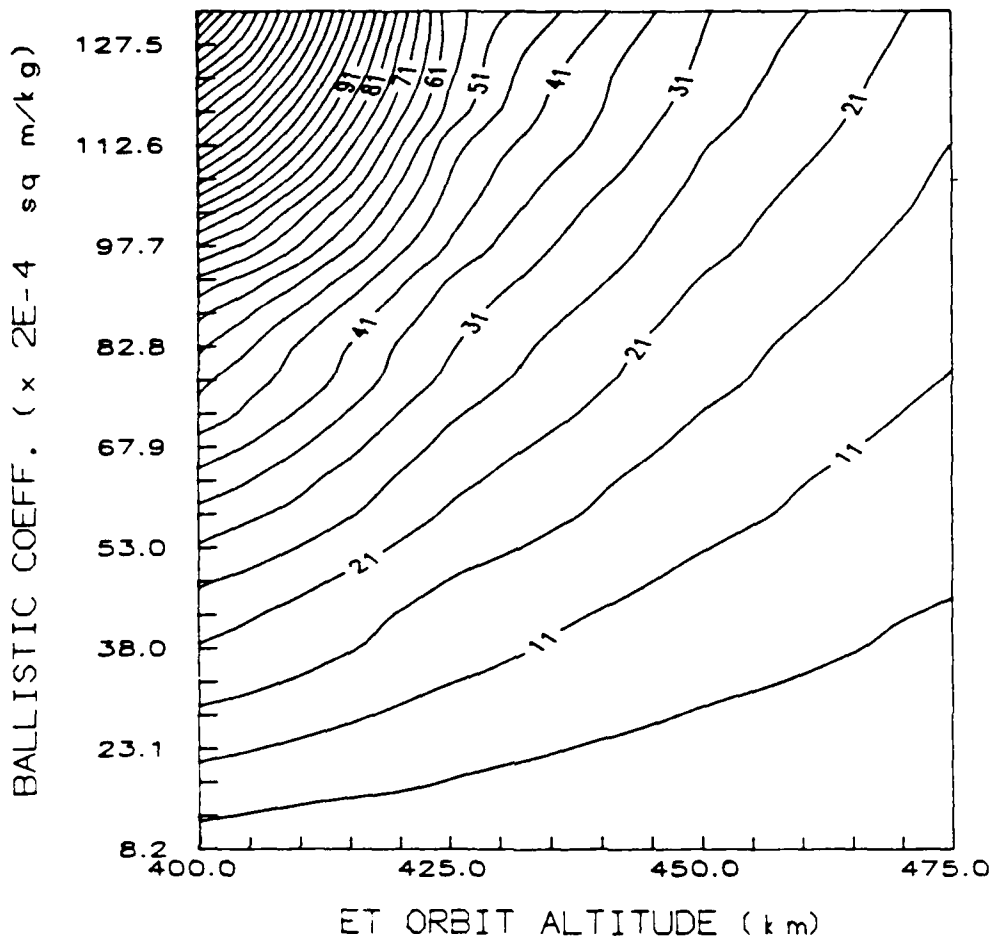


Figure 19. Contour Graph of 90-Day Altitude Loss

Third Body Effects

Since the Artificial Satellite Analysis Program has the capability to include third body perturbations, an investigation was conducted to determine if the Sun or Moon would have any effect on an orbiting External Tank. Test cases were performed with the standard orbit of 28° inclination, zero eccentricity and an initial altitudes of 425 km. Both

Earth's gravitational and atmospheric perturbations were included. The third body situations explored were: Sun only, Moon only and Sun/Moon together. Table IV lists the curve fitting polynomials calculated for the Sun/Moon computer run. No noticeable differences were found between the orbit histories produced here and the like profile accomplished in the first section of the results.

TABLE IV

Orbit Element Polynomials for Sun/Moon Effects

$$a = 6801.2284434 - 0.2122904 t - 0.0003230 t^2$$

$$e = 0.0012659 + 0.0000010 t$$

$$i = 27.9840822 - 0.0000204 t$$

$$\Omega = 360.1587464 - 7.0663866 t$$

$$\text{Geo.Alt.} = 417.1945712 - 0.2459292 t$$

VI. Conclusions and Recommendations

Conclusions

This orbital analysis of an External Tank in low Earth orbit represents a 'first look' at how the tank would react to the perturbative effects of Earth's gravitational field and atmosphere. A scenario involving an ET parking orbit was developed as a way to limit the scope of the problem. The gravity gradient attitude, the coefficient of drag and the simple atmosphere model were the major assumptions to this investigation.

A major outcome of this study was the 425 km altitude, determined to be the lowest initial altitude for keeping the External Tank in the specified parking orbit. Under the presumptions used in the scenario, the ET lost approximately 22 km during the 90-day period examined. The 425 km altitude is within reach of the Shuttle/ET combination (5:2), thus no ET reboost would be necessary under these stated conditions.

Due to the daily variations in the calculated orbital elements a curve fitting program was used to extract their long term behavior. In this process the Artificial Satellite Analysis Program generated the time histories of the orbital elements and an 'averaging' was then performed. The polynomials produced by using ASAP output data provide a

quick method of determining future values of the External Tank orbital elements.

From this initial study of an External Tank in space, several conclusions can be drawn from the long period trends in the ET's orbital parameters. As with all satellites in LEO, the atmosphere causes the semi-major axis to shrink at an ever increasing rate. When deposited in orbit with zero eccentricity, the ET will remain in a near circular orbit. The inclination of its orbit will also stay close to initial conditions. The orientation of the ET orbital plane, as defined by the longitude of ascending node, cycles approximately every 50 days. Any rendezvous missions with an on-orbit External Tank will have to take this into account.

The examination of the various factors that influence the External Tank orbit decay rate showed that some factors are more detrimental than others. The ET inclination and eccentricity parameters, within the nominal Shuttle operating limits, have minor effects on orbit contraction. On the other hand, the 3-dimensional graph and associated contour plot (Figures 18 and 19) demonstrate the combined effects of atmospheric density and ET characteristics of area, mass, and drag coefficient. At lower altitudes where the air density is greater, small increases in the ballistic coefficient produce large changes in the altitude lost by the External Tank during the 90-day period.

The Earth's gravity field cannot be neglected in an analysis of an orbiting External Tank. The gravitational and atmospheric drag perturbations interact to produce a greater altitude loss than their individual effects. However, for a long term orbital study, the short period gravitation anomalies can be disregarded since a 2x0 field that models Earth's oblateness can provide sufficient accuracy.

Recommendations

As with any initial study into a problem, follow-on work is appropriate. Several diverse areas could be examined for greater insight into an orbiting External Tank. As modelled, the atmosphere used in this thesis was one of the simplest possible. It would be beneficial to employ a dynamic model where the time dependence of the atmospheric properties is considered. To be on the conservative side this study started the ET in a gravity gradient position which presented the largest possible area to the air flow. At some point in the ET's orbit decay, moments due to aerodynamic forces will become the predominant torque on the tank and it will then transition from a stabilized orientation into an uncontrollable state. An investigation into the ET's orbit dynamics would provide a more accurate value for its projected area. Also, an analysis could be accomplished to determine the amount of lift generated by the ET and the effect on orbital contraction.

In addition to this projected area another uncertainty is the External Tank's coefficient of drag. The value of C_d is dependent on the accommodation coefficient where the interaction of the air molecules with a satellite's surface plays an important part. However, a foam covered ET presents quite a different exterior to the atmospheric flow than the normal metallic surfaces of other spacecraft. An examination into this area could result in different values of the drag coefficient being appropriate for use in an ET orbital analysis. As emphasized earlier, even small changes in these External Tank characteristics can have considerable influence in the orbital decay rate.

The possibility exists that multiple External Tanks could be stored in an orbiting 'tank farm' (Figure 20).

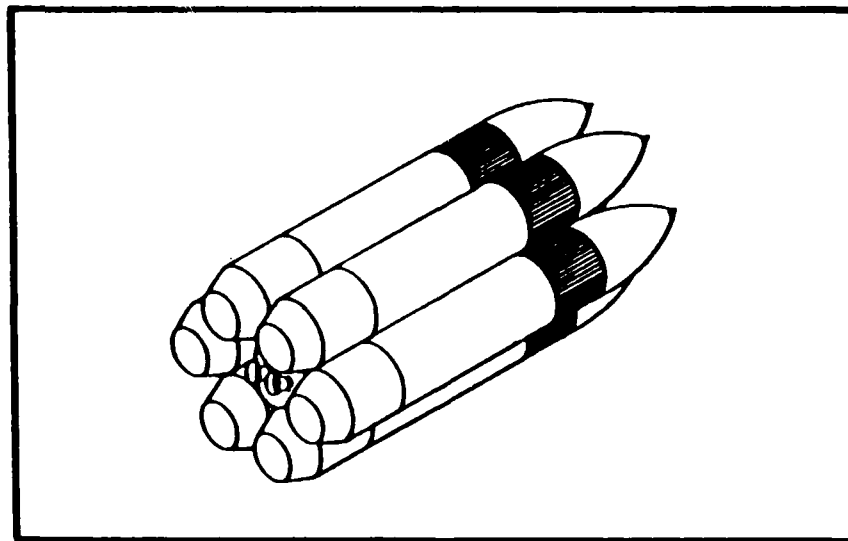


Figure 20. Multiple External Tanks

Looking at the drag deceleration equation

$$\frac{D}{m} = \frac{C_d A}{2m} \rho V^2 \quad (21)$$

the magnitude of the deceleration could be decreased by the proper orientation of two or more tanks. It may be possible to fix the attitude of the multiple tanks so the increase in the area exposed to the air flow is more than offset by the increased tank mass. However, an analysis of multi-tank drag coefficients would be required first.

Another possible avenue of study would be to develop the method of averages analytical technique discussed in Chapter III to include both gravitational and atmospheric drag perturbations. A comparasion could then be done between this technique and the approach followed by this thesis.

The proposed uses of an orbiting External Tank bolster the idea that it is too valuable a resource to be expended on each Space Shuttle flight. The United States has previously adapted other space hardware for new applications. The prime example of this flexibility is Skylab, where a third stage from a Saturn V was converted into a space station. But, like Skylab, an External Tank will not stay in orbit indefinitely. Plans and decisions must be made prior to its use in space. This thesis has attempted to provide some preliminary answers to this problem.

Appendix A

Conversion of the Spherical Harmonic to Keplerian Elements

This section will be concerned with transforming the expression for the geopotential discussed in Chapter III into a form that can be used in the method of averages and is developed mainly from References 2 and 14. The potential is a function of radius r , latitude ϕ and longitude λ :

$$V = \sum_{l=0}^{\infty} \sum_{m=0}^l r^{-l-1} P_{lm}(\sin\phi) \left[C_{lm} \cos m\lambda + S_{lm} \sin m\lambda \right] \quad (1)$$

This equation involves an associated Legendre function:

$$P_{lm}(\sin\phi) = \cos^m\phi \sum_{t=0}^k T_{lmt} \sin^{l-m-2t}\phi \quad (2)$$

where $k = \text{integer part of } (l-m)/2 \text{ and}$

$$T_{lmt} = \frac{(-1)^t (2l-2t)!}{2^l t! (l-t)! (l-m-2t)!} \quad (3)$$

For use in the method of averages this potential needs to be converted to the Keplerian elements a, e, i, Ω, ω and m .

To accomplish this element transformation several trigonometric identities will be required:

$$\begin{aligned} \cos mx &= \operatorname{Re} \sum_{s=0}^m \binom{m}{s} j^s \cos^{m-s}x \sin^s x \\ \sin mx &= \operatorname{Re} \sum_{s=0}^m \binom{m}{s} j^{s-1} \cos^{m-s}x \sin^s x \end{aligned} \quad (4)$$

where

Re \equiv real part

$$j \equiv \sqrt{-1}$$

$$\begin{pmatrix} m \\ s \end{pmatrix} \equiv \frac{m!}{s! (m-s)!}$$

The notation $\begin{pmatrix} m \\ s \end{pmatrix}$ is referred to in literature as the Binomial Coefficient. Also,

$$\sin^a x \cos^b x = \frac{(-1)^a j^a}{2^{a+b}} \sum_{c=0}^a \sum_{d=0}^b \begin{pmatrix} a \\ c \end{pmatrix} \begin{pmatrix} b \\ d \end{pmatrix} (-1)^c X [\cos(a+b-2c-2d)x + j \sin(a+b-2c-2d)x] \quad (5)$$

and

$$\begin{aligned} \cos a \cos b &= 1/2 [\cos(a+b) + \cos(a-b)] \\ \sin a \sin b &= 1/2 [\cos(a-b) - \cos(a+b)] \\ \sin a \cos b &= 1/2 [\sin(a-b) + \sin(a+b)] \\ \cos a \sin b &= 1/2 [\sin(a+b) - \sin(a-b)] \end{aligned} \quad (6)$$

One term of the potential series can be represented as

$$V_{lm} = \frac{\mu a_e^l}{r^{l+1}} P_{lm}(\sin\phi) [C_{lm} \cos m\lambda + S_{lm} \sin m\lambda] \quad (7)$$

The factor μa_e^l non-dimensionalizes the coefficients C_{lm} and S_{lm} where a_e is the equatorial radius of body M.

Working with Figure 21 a substitution is now made for $m\lambda$,

$$m\lambda = [m(\alpha - \Omega) + m(\Omega - \theta)] \quad (8)$$

where α is the right ascension and θ is Greenwich sidereal time; i.e. $\lambda = \alpha - \theta$. This produces

$$\begin{aligned} \cos m\lambda &= \cos m(\alpha - \Omega) \cos m(\Omega - \theta) - \sin m(\alpha - \Omega) \sin m(\Omega - \theta) \\ \sin m\lambda &= \sin m(\alpha - \Omega) \cos m(\Omega - \theta) + \cos m(\alpha - \Omega) \sin m(\Omega - \theta) \end{aligned} \quad (9)$$

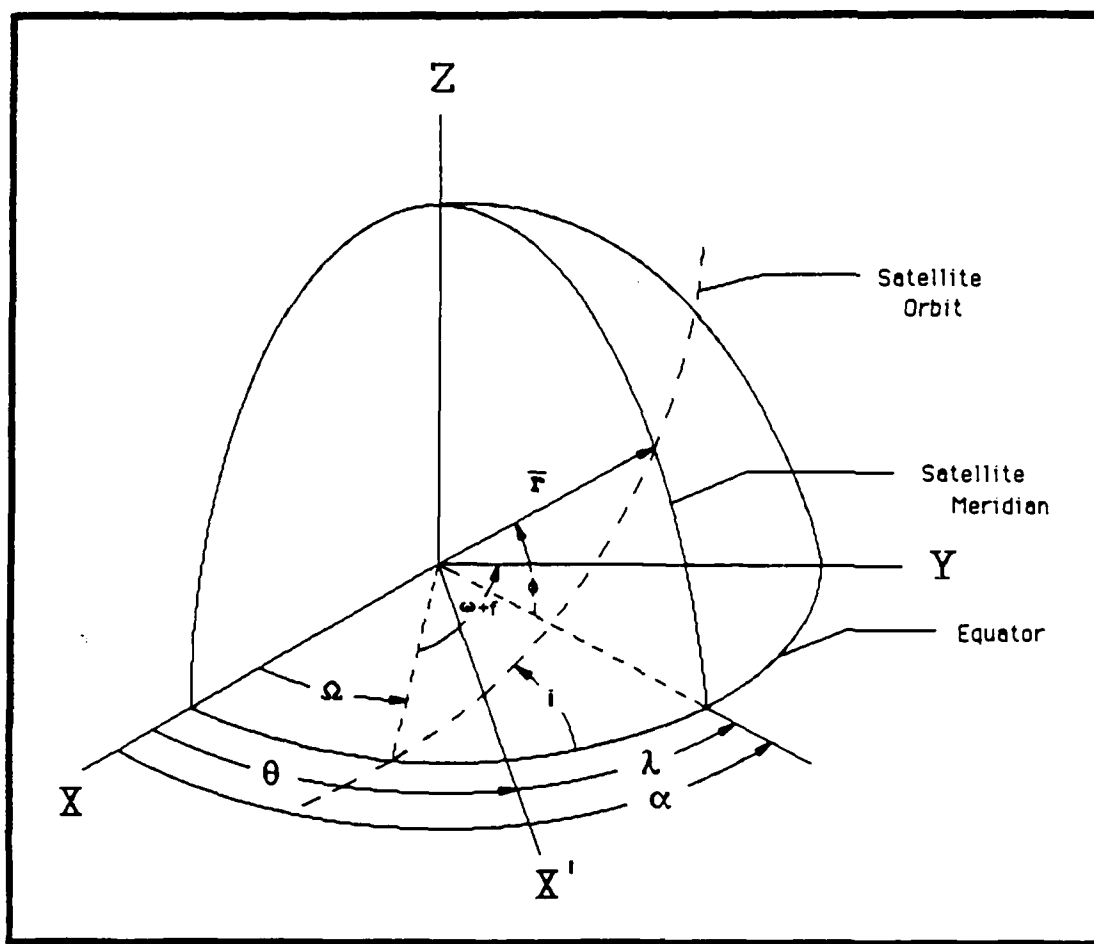


Figure 21. Satellite Orbital Elements

Using spherical trigonometric relationships from Figure 21

$$\cos (\omega+f) = \cos (\alpha-\Omega) \cos \phi + \sin (\alpha-\Omega) \sin \phi \cos \pi / 2 \quad (10)$$

$$\cos \phi = \cos (\omega+f) \cos (\alpha-\Omega) + \sin (\omega+f) \sin (\alpha-\Omega) \cos i \quad (11)$$

where f is the true anomaly.

From Eqs (10) and (11) come

$$\cos (\alpha-\Omega) = \cos (\omega+f) / \cos \phi \quad (12a)$$

$$\sin (\alpha-\Omega) = \sin (\omega+f) \cos i / \cos \phi \quad (12b)$$

$$\sin \phi = \sin i \sin (\omega+f) \quad (13)$$

Now; trigonometric identities (4) are applied to Eqs (9) and identities (12) are substituted into the result. These steps yield

$$\begin{aligned}\cos m\lambda &= \operatorname{Re} \sum_{s=0}^m \binom{m}{s} j^s \frac{\cos^{m-s}(\omega+f) \sin^s(\omega+f) \cos^s i}{\cos^m \phi} \\ &\quad \times [\cos m(\Omega-\theta) + j \sin m(\Omega-\theta)] \\ \sin m\lambda &= \operatorname{Re} \sum_{s=0}^m \binom{m}{s} j^s \frac{\cos^{m-s}(\omega+f) \sin^s(\omega+f) \cos^s i}{\cos^m \phi} \\ &\quad \times [\sin m(\Omega-\theta) - j \cos m(\Omega-\theta)] \quad (14)\end{aligned}$$

The terms on the right side of Eq (13) are substituted for $\sin \phi$ into the associated Legendre function Eq (2). This new P_{lm} with Eqs (14) are then placed into the potential Eq (7) to give

$$\begin{aligned}V_{lm} &= \frac{\mu a_e^l}{r^{l+1}} \sum_{t=0}^k T_{lmt} \sin^{l-m-2t} i \operatorname{Re} \left\{ \left[\left[C_{lm} - j S_{lm} \right] \cos m(\Omega-\theta) \right. \right. \\ &\quad \left. \left. + \left[S_{lm} + j C_{lm} \right] \sin m(\Omega-\theta) \right] \sum_{s=0}^m \binom{m}{s} j^s \sin^{l-m-2t+s}(\omega+f) \right. \\ &\quad \left. \left. \cos^{m-s}(\omega+f) \cos^s i \right\} \quad (15)\end{aligned}$$

where k is the integer part of $(l-m)/2$. Identity (5) along with the substitutions $a = l-m-2t+s$ and $b = m-s$ produce

$$V_{lm} = \frac{\mu a_e^l}{r^{l+1}} \sum_{t=0}^k T_{lmt} \sin^{l-m-2t} i \operatorname{Re} \left[\left[C_{lm} - jS_{lm} \right] \cos m(\Omega - \theta) \right. \\ \left. + \left[S_{lm} + jC_{lm} \right] \sin m(\Omega - \theta) \right] \sum_{s=0}^m \binom{m}{s} j^s \cos^s i \frac{(-j)^{-m-2t+s}}{2^{l-2t}}$$

$$\times \sum_{c=0}^{l-m-2t+s} \sum_{d=0}^{m-s} \binom{l-m-2t+s}{c} \binom{m-s}{d} (-1)^c$$

$$\times [\cos(l-2t-2c-2d)(\omega+f) + j \sin(l-2t-2c-2d)(\omega+f)] \quad (16)$$

Applying identities (6) to products of trigonometric functions in Eq (16) and neglecting any term with an odd power of j (since V_{lm} is real) results in

$$V_{lm} = \frac{\mu a_e^l}{r^{l+1}} \sum_{t=0}^k T_{lmt} \sin^{l-m-2t} i (-1)^{k+t} \sum_{s=0}^m \binom{m}{s} \frac{\cos^s i}{2^{l-2t}}$$

$$\times \sum_{c=0}^{l-m-2t+s} \sum_{d=0}^{m-s} \binom{l-m-2t+s}{c} \binom{m-s}{d} (-1)^c$$

$$\times \left\{ \begin{array}{l} \left[C_{lm} \right]_{l-m \text{ even}} \\ \left[-S_{lm} \right]_{l-m \text{ odd}} \end{array} \cos [(l-2t-2c-2d)(\omega+f) + m(\Omega - \theta)] \right. \\ \left. + \begin{array}{l} \left[S_{lm} \right]_{l-m \text{ even}} \\ \left[C_{lm} \right]_{l-m \text{ odd}} \end{array} \sin [(l-2t-2c-2d)(\omega+f) + m(\Omega - \theta)] \right\} \quad (17)$$

Next, letting $p = (t+c+d)$ produces

$$V_{lm} = \frac{\mu a_e^l}{r^{l+1}} \sum_{p=0}^l F_{lmp}(i) \left\{ \begin{aligned} &\left[\begin{matrix} C_{lm} \\ -S_{lm} \end{matrix} \right]_{l-m \text{ odd}}^{l-m \text{ even}} \cos [(1-2p)(\omega+f) + m(\Omega-\theta)] \\ &+ \left[\begin{matrix} S_{lm} \\ C_{lm} \end{matrix} \right]_{l-m \text{ odd}}^{l-m \text{ even}} \sin [(1-2p)(\omega+f) + m(\Omega-\theta)] \end{aligned} \right\} \quad (18)$$

where $F_{lmp}(i)$ is the Inclination function

$$F_{lmp}(i) = \sum_t \frac{(2l-2t)!}{t! (l-t)! (l-m-2t)! 2^{2l-2t}} \sin^{l-m-2t} i$$

$$\times \sum_{s=0}^m \binom{m}{s} \cos^s i \sum_c \binom{l-m-2t+s}{c} \binom{m-s}{p-t-c} (-1)^{c-k} \quad (19)$$

where k is the integer part of $(l-m)/2$. Also, t is summed from zero to the lessor of p or k and c is summed over all values making the binomial coefficients nonzero. These summations for t and c are due to the definition of the Binomial Coefficient. The lower term in the coefficient must be equal to or greater than zero and the upper term must be equal to or greater than the lower term.

At this point the potential equation still depends on the radius r and the true anomaly f . These coordinates can be replaced with the semi-major axis a , eccentricity e and mean anomaly M . Extracting the general trigonometric term from Eq (18) yields

$$\frac{1}{r^{l+1}} \begin{bmatrix} \cos \\ \sin \end{bmatrix} [(l-2p)\omega + m(\Omega - \theta)] + m(\Omega - \theta) \quad (20)$$

where the notation $\begin{bmatrix} \cos \\ \sin \end{bmatrix}$ means that both sine and cosine terms will be present in the expression. Letting $\epsilon = (l-2p)\omega + m(\Omega - \theta)$ and using the trig addition formulas, Eq (20) becomes

$$\frac{1}{r^{l+1}} \begin{bmatrix} \cos (l-2p)f \cos \epsilon - \sin (l-2p)f \sin \epsilon \\ \sin (l-2p)f \cos \epsilon + \cos (l-2p)f \sin \epsilon \end{bmatrix} \quad (21)$$

The terms $\left(\frac{r}{a}\right)^n \cos mf$ and $\left(\frac{r}{a}\right)^n \sin mf$ can be developed into a Fourier series in M :

$$\begin{aligned} \left(\frac{r}{a}\right)^n \cos mf &= \sum_{t=-\infty}^{\infty} X_t^{n,m} \cos tM \\ \left(\frac{r}{a}\right)^n \sin mf &= \sum_{t=-\infty}^{\infty} X_t^{n,m} \sin tM \end{aligned} \quad (22)$$

where $X_t^{n,m}$ are called Hansen's coefficients. Substituting Eqs (22) (with $t = l-2p+q$, $m = l-2p$ and $n = -l-1$) into expression (21) yields

$$\frac{1}{a^{l+1}} \begin{bmatrix} \sum_{q=-\infty}^{\infty} X_{l-2p+q}^{-l-1, l-2p} [\cos (l-2p+q)M \cos \epsilon - \sin (l-2p+q)M \sin \epsilon] \\ \sum_{q=-\infty}^{\infty} X_{l-2p+q}^{-l-1, l-2p} [\sin (l-2p+q)M \cos \epsilon + \cos (l-2p+q)M \sin \epsilon] \end{bmatrix} \quad (23)$$

From this, the general term (20) becomes

$$\frac{1}{a^{1+1}} \sum_{q=-\infty}^{\infty} X_{1-2p+q}^{-1-1, 1-2p} \begin{bmatrix} \cos \\ \sin \end{bmatrix} [(1-2p)\omega + (1-2p+q)M + m(\Omega-\theta)] \quad (24)$$

Determining Hansen's coefficients, $X_t^{n,m}$, is quite an involved process. Their development can be found in Reference 1.

The coefficients, $X_{1-2p+q}^{-1-1, 1-2p}$, are dependent on eccentricity alone so an Eccentricity function $G_{1pq}(e)$ can be defined:

$$\begin{aligned} X_{1-2p+q}^{-1-1, 1-2p} &= G_{1pq}(e) \\ &= (-1)^{|q|} (1+\beta^2)^{-1} \beta^{|q|} \sum_{k=0}^{\infty} P_{1pqk} Q_{1pqk} \beta^{2k} \end{aligned} \quad (25)$$

where

$$\beta = \frac{e}{1 + \sqrt{1-e^2}} = \frac{1 - \sqrt{1-e^2}}{e} \quad (26)$$

$$\text{and} \quad P_{1pqk} = \sum_{r=0}^h \begin{bmatrix} 2p'-2l \\ h-r \end{bmatrix} \frac{(-1)^r}{r!} \left(\frac{(1-2p'+q') e}{2\beta} \right)^r \quad (27)$$

$$\begin{aligned} \text{where} \quad h &= k + q' \quad \text{for } q' > 0 \\ h &= k \quad \text{for } q' < 0 \end{aligned}$$

$$\text{and} \quad Q_{1pqk} = \sum_{r=0}^n \begin{bmatrix} -2p' \\ n-r \end{bmatrix} \frac{1}{r!} \left(\frac{(1-2p'+q') e}{2\beta} \right)^r \quad (28)$$

$$\begin{aligned} \text{where} \quad n &= k \quad \text{for } q' > 0 \\ n &= k - q' \quad \text{for } q' < 0 \end{aligned}$$

$$\begin{aligned} \text{with} \quad p' &= p, \quad q' = q \quad \text{if } p \leq 1/2 \\ p' &= 1-p, \quad q' = -q \quad \text{if } p > 1/2 \end{aligned}$$

At this point, with the preceding definition for Hansen's coefficients, the general term (24) can be inserted back into the potential equation (18) producing

$$V_{lm} = \frac{\mu a_e^l}{a^{l+1}} \sum_{p=0}^l F_{lmp}(i) \sum_{q=-\infty}^{\infty} G_{lpq}(e) S_{lmpq}(\omega, M, \Omega, \theta) \quad (29)$$

where

$$S_{lmpq} = \begin{bmatrix} C_{lm} \\ -S_{lm} \end{bmatrix}_{l-m \text{ even}}^{l-m \text{ odd}} \cos [(1-2p)\omega + (1-2p+q)M + m(\Omega-\theta)] \\ + \begin{bmatrix} S_{lm} \\ C_{lm} \end{bmatrix}_{l-m \text{ even}}^{l-m \text{ odd}} \sin [(1-2p)\omega + (1-2p+q)M + m(\Omega-\theta)] \quad (30)$$

A table of $F_{lmp}(i)$ and $G_{lpq}(e)$ functions is given in Reference 14. This completes the transformation of the potential from spherical to Keplerian coordinates. At this stage, the geopotential V could be averaged over one orbital period (12:3-4):

$$\langle V_{ave} \rangle = \frac{1}{2\pi} \int_0^{2\pi} V(M) dM \quad (31)$$

This would eliminate any dependence of Eq (1) on the mean anomaly and remove all short-term variations from this disturbing function and subsequently, from the equations of motion.

Appendix B

Orbital Element Polynomials

The following polynomials were generated from External Tank orbit data calculated by the Artificial Satellite Analysis Program at initial altitudes of: 400, 425, 450, 475 and 500 kilometers.

400 km

$$\begin{aligned}a &= 6775.9368930 - 0.2960781 t - 0.0014187 t^2 \\e &= 0.0013940 - 0.0000023 t \\i &= 27.9842948 - 0.0000305 t \\\Omega &= 360.2713382 - 7.1702218 t \\\text{Geo.Alt} &= 391.4884943 - 0.3029662 t - 0.0013949 t^2\end{aligned}$$

425 km

$$\begin{aligned}a &= 6801.2279327 - 0.2122813 t - 0.0003232 t^2 \\e &= 0.0012661 + 0.0000010 t \\i &= 27.9844744 - 0.0000193 t \\\Omega &= 360.1578150 - 7.0659969 t \\\text{Geo.Alt} &= 417.1935674 - 0.2159279 t\end{aligned}$$

450 km

$$\begin{aligned}a &= 6825.9871108 - 0.1213986 t - 0.0003565 t^2 \\e &= 0.0014040 - 0.0000010 t \\i &= 27.9858543 - 0.0000615 t \\\Omega &= 360.1058726 - 6.9688603 t \\\text{Geo.Alt} &= 441.8590712 - 0.1519032 t\end{aligned}$$

475 km

$$a = 6851.2169711 - 0.0949190 \text{ t}$$

$$e = 0.0013932 - 0.0000004 \text{ t}$$

$$i = 27.9846431 - 0.0000141 \text{ t}$$

$$\Omega = 360.0663384 - 6.8757352 \text{ t}$$

$$\text{Geo.Alt.} = 466.7700440 - 0.0982593 \text{ t}$$

500 km

$$a = 6876.1566632 - 0.0619361 \text{ t}$$

$$e = 0.0013675 + 0.0000002 \text{ t}$$

$$i = 27.9848512 - 0.0000140 \text{ t}$$

$$\Omega = 360.0416657 - 6.7857346 \text{ t}$$

$$\text{Geo.Alt} = 491.7578786 - 0.0658334 \text{ t}$$

Bibliography

1. Bain, Rodney D. Lecture material from Advanced Astrodynamics II. School of Engineering, Air Force Institute of Technology (AU), Wright-Patterson AFB OH, January 1987.
2. Born, George H. and Claude E. Hildebrande, Jr. The Conversion of the Spherical Harmonic and Third Body Potential to Keplerian Elements. Contract 9-2619. NASA Manned Spacecraft Center, May 1967.
3. Cook, G.E. "Satellite Drag Coefficients," Planetary and Space Science, 13: 929-946 (October 1965).
4. Dowd, Douglas L. and B. D. Tapley. "Density Models for the Upper Atmosphere," Celestial Mechanics, 20: 271-295 (October 1979).
5. "External Tank Utilization on Orbit," Space Studies Institute Update, 13: 1-3 (July/August 1987).
6. Fitzpatrick, Philip M. Principles of Celestial Mechanics. New York: Academic Press, Inc. 1970.
7. Gerald, Curtis F. Applied Numerical Analysis (Second Edition). Reading, MA: Addison-Wesling Publishing Company, 1980.
8. Gimarc, Alex J. Report on Space Shuttle External Tank Application. Space Studies Institute, Princeton, NJ, December 1985.
9. Jacchia, Luigi G. "Variations in the Earth's Upper Atmosphere as Revealed by Satellite Drag," Reviews of Modern Physics, 35: 973-991 (October 1963).
10. Jane's Spaceflight Directory (Second Edition). London: Jane's, 1986.
11. Jenson, Jorgen and others. Design Guide to Orbital Flight. New York: McGraw-Hill Book Company, 1962.
12. Johnson, Francis S., ed. Satellite Environment Handbook. Stanford, CA: Stanford University Press, 1965.

13. Kaufman, Bernard. "Variation of Parameters and the Long-Term Behavior of Planetary Orbiters," AIAA Paper No. 70-1055, AAS/AIAA Astronautics Conference, 1-3 August 1970.
14. Kaula, William M. Theory of Satellite Geodesy. Waltham, MA: Blaisdell Publishing Company, 1966.
15. King-Hele, Desmond. Theory of Satellite Orbits in an Atmosphere. London: Butterworths, 1961.
16. Kwok, Johnny H. The Artificial Satellite Analysis Program (ASAP). Jet Propulsion Laboratory, 1 April 1985.
17. Martin Marietta Michoud Aerospace. External Tank Gamma Ray Imaging Telescope Study. Contract NAS8-36394, January 1987.
18. Meirovitch, L. and F. B. Wallace, Jr. "On the Effect of Aerodynamic and Gravitational Torques on the Attitude Stability of Satellites," AIAA Journal, 4: 2196-2202 (December 1966).
19. National Aeronautics and Space Administration. Spacecraft Aerodynamic Torques. NASA SP-8058. January 1971.
20. National Oceanic and Atmospheric Administration. U.S. Standard Atmosphere, 1976. Washington: NOAA, October 1976.
21. Regan, Frank J. Re-Entry Vehicle Dynamics. New York: American Institute of Aeronautics and Astronautics, Inc., 1984.
22. Roy, Archie E. The Foundations of Astronautics. New York: Macmillan, 1965.
23. Sentman, Lee H. and Stanford E. Neice. "Drag Coefficients for Tumbling Satellites," Journal of Spacecraft and Rockets, 4: 1270-1272 (September 1967).
24. Silberberg, Rein and others. "Radiation Hazards in Space," Aerospace America, 25: 38-41 (October 1987).
25. Taff, Laurence G. Celestial Mechanics, A Computational Guide for the Practitioner. New York: John-Wiley & Sons, 1985.
26. Vaughn, Robert L., ed., Space Shuttle, A Triumph in Manufacturing. Dearborn, MI: Society of Manufacturing Engineers, 1985.

27. Viñu, Nguyen X. and others. Hypersonic and Planetary Entry Flight Mechanics. Ann Arbor, MI: The University of Michigan Press, 1980.
28. Weisel, William E. Lecture material from MC636, Advanced Astrodynamics. School of Engineering, Air Force Institute of Technology (AU), Wright-Patterson AFB OH, January 1987.
29. Wiggins, Lyle E. "Relative Magnitudes of the Space-Environmental Torques on a Satellite," AIAA Journal, 2: 770-771 (December 1966).
30. Williams, Richard R. "Drag Coefficients for Astronomical Observatory Satellites," Journal Of Spacecraft and Rockets, 12: 74-78 (February 1975).

VITA

Major Dennis D. Miner was born on 2 January 1952 in Bremerhaven, Germany. He graduated from Lake Taylor High School in Norfolk, Virginia in 1970. He then attended Purdue University on a four-year ROTC scholarship and graduated in May 1974 with a Bachelor of Science degree in Aeronautical and Astronautical Engineering. After graduation, he worked as an aeronautical engineer with NASA at the Langley Research Center. Major Miner started active duty in November 1974 and entered Undergraduate Pilot Training at Reese AFB, Texas. After receiving his wings, he was stationed at Homestead AFB, Florida for F-4 training. His next two operational assignments were with the 70th Tactical Fighter Squadron at Moody AFB, Georgia and the 57th Fighter Interceptor Squadron in Keflavik, Iceland. Upon the completion of his remote tour, he returned to Homestead AFB in February 1979 as an F-4 Instructor Pilot with the 306th Tactical Fighter Training Squadron. Prior to coming to the Air Force Institute of Technology in May 1986, Major Miner was a flight commander with the 64th Aggressor Squadron at Nellis AFB, Nevada.

Permanent Address: 2419 Jasper Court
Norfolk, VA 23518

REPORT DOCUMENTATION PAGE

Form Approved
OMB No. 0704-0188

1a. REPORT SECURITY CLASSIFICATION UNCLASSIFIED			1b. RESTRICTIVE MARKINGS		
2a. SECURITY CLASSIFICATION AUTHORITY			3. DISTRIBUTION/AVAILABILITY OF REPORT Approved for Public Release Distribution Unlimited		
2b. DECLASSIFICATION/DOWNGRADING SCHEDULE					
4. PERFORMING ORGANIZATION REPORT NUMBER(S) AFIT/GA/AA/87D-4			5. MONITORING ORGANIZATION REPORT NUMBER(S)		
6a. NAME OF PERFORMING ORGANIZATION School of Engineering		6b. OFFICE SYMBOL (If applicable) AFIT/ENY		7a. NAME OF MONITORING ORGANIZATION	
6c. ADDRESS (City, State, and ZIP Code) Air Force Institute of Technology (AU) Wright-Patterson AFB, OH 45433-6583			7b. ADDRESS (City, State, and ZIP Code)		
8a. NAME OF FUNDING/SPONSORING ORGANIZATION		8b. OFFICE SYMBOL (If applicable)		9. PROCUREMENT INSTRUMENT IDENTIFICATION NUMBER	
8c. ADDRESS (City, State, and ZIP Code)			10. SOURCE OF FUNDING NUMBERS		
		PROGRAM ELEMENT NO.		PROJECT NO.	TASK NO.
				WORK UNIT ACCESSION NO.	
11. TITLE (Include Security Classification) ORBITAL ANALYSIS OF A STS EXTERNAL TANK IN LOW EARTH ORBIT					
12. PERSONAL AUTHOR(S) Dennis D. Miner, B.S., Major, USAF					
13a. TYPE OF REPORT MS Thesis		13b. TIME COVERED FROM _____ TO _____		14. DATE OF REPORT (Year, Month, Day) 1987 December	
15. PAGE COUNT 81					
16. SUPPLEMENTARY NOTATION					
17. COSATI CODES			18. SUBJECT TERMS (Continue on reverse if necessary and identify by block number)		
FIELD	GROUP	SUB-GROUP			
22	03		External Tank, Trajectory Analysis, Satellite Orbits, Satellite Drag, Gravitational Perturbations, Orbital Elements		
19. ABSTRACT (Continue on reverse if necessary and identify by block number) Thesis Chairman: Rodney D. Bain, Captain, USAF Instructor of Astronautical Engineering					
20. DISTRIBUTION STATEMENT (For Public Release Only) <input checked="" type="checkbox"/> UNCLASSIFIED			21. ABSTRACT SECURITY CLASSIFICATION UNCLASSIFIED		
22a. NAME OF REPORTING ORGANIZATION Rodney D. Bain, Captain, USAF			22b. NAME OF MONITORING ORGANIZATION AFIT/ENY		

Abstract

By flying a different launch profile , it is possible for the Space Transportation System's Orbiter to bring the External Tank directly into space. Many studies by NASA and private industry have detailed the potential on-orbit uses of an External Tank. However, at Space Shuttle operating altitudes, an orbiting tank will experience multiple environmental forces resulting in its decay into the lower atmosphere and eventual re-entry.

This thesis conducts a preliminary study of a single External Tank in low Earth orbit. Criteria for a parking orbit are defined and, using an orbit prediction computer program with atmospheric drag and gravitational perturbations included, a search is made for the lowest initial altitude that will allow the External Tank to remain in this orbit window. The starting altitude that meets the orbit requirements is found to be within reach of the Shuttle's capabilities. The orbital elements of this parking orbit are then analyzed and a method for quick calculation of these parameters is devised. An evaluation of the factors that affect the orbital contraction of an External Tank is also performed. The atmospheric density and the tank characteristics can both contribute to high orbital decay rates.

END

FILMED

MARCH, 19 88

DTIC